

**NASA
SPACE VEHICLE
DESIGN CRITERIA
(STRUCTURES)**

NASA SP-8066

DEPLOYABLE AERODYNAMIC DECELERATION SYSTEMS



**CASE FILE
COPY**

JUNE 1971

NATIONAL AERONAUTICS AND SPACE ADMINISTRATION

FOREWORD

NASA experience has indicated a need for uniform criteria for the design of space vehicles. Accordingly, criteria are being developed in the following areas of technology:

Environment
Structures
Guidance and Control
Chemical Propulsion

Individual components of this work will be issued as separate monographs as soon as they are completed. A list of all published monographs in this series can be found at the end of this document.

These monographs are to be regarded as *guides* to the formulation of design requirements by NASA Centers and project offices.

This monograph was prepared under the cognizance of the Langley Research Center. The Task Manager was J. R. Hall. The author was E. G. Ewing of Northrop Corporation. Other individuals assisted in the development and review. In particular, significant contributions made by R. J. Berndt of U.S. Air Force Flight Dynamics Laboratory; J. M. Brayshaw of Jet Propulsion Laboratory; D. R. Casper and W. J. Chagaris of McDonnell Douglas Corporation; H. Elksnin, C. L. Gillis, J. C. McFall, Jr., M. M. Mikulas, Jr., and H. N. Murrow of NASA Langley Research Center; E. J. Giebotowski of U.S. Army Natick Laboratories; J. W. Kiker of NASA Manned Spacecraft Center; R. A. Pohl of Raven Industries, Inc.; F. R. Nebiker of Goodyear Aerospace Corporation; J. D. Nicolaides of University of Notre Dame; J. D. Reuter of Pioneer Parachute Company; and O. W. Sepp of M. Steinthal and Son, Inc., are hereby acknowledged.

NASA plans to update this monograph when need is established. Comments and recommended changes in the technical content are invited and should be forwarded to the attention of the Design Criteria Office, Langley Research Center, Hampton, Virginia 23365.

June 1971

For sale by the National Technical Information Service, Springfield, Virginia 22151 – Price \$3.00

GUIDE TO THE USE OF THIS MONOGRAPH

The purpose of this monograph is to provide a uniform basis for design of flightworthy structure. It summarizes for use in space vehicle development the significant experience and knowledge accumulated in research, development, and operational programs to date. It can be used to improve consistency in design, efficiency of the design effort, and confidence in the structure. All monographs in this series employ the same basic format – three major sections preceded by a brief INTRODUCTION, Section 1, and complemented by a list of REFERENCES.

The STATE OF THE ART, Section 2, reviews and assesses current design practices and identifies important aspects of the present state of technology. Selected references are cited to supply supporting information. This section serves as a survey of the subject that provides background material and prepares a proper technological base for the CRITERIA and RECOMMENDED PRACTICES.

The CRITERIA, Section 3, state *what* rules, guides, or limitations must be imposed to ensure flightworthiness. The criteria can serve as a checklist for guiding a design or assessing its adequacy.

The RECOMMENDED PRACTICES, Section 4, state *how* to satisfy the criteria. Whenever possible, the best procedure is described; when this cannot be done, appropriate references are suggested. These practices, in conjunction with the criteria, provide guidance to the formulation of requirements for vehicle design and evaluation.

CONTENTS

1.	INTRODUCTION	1
2.	STATE OF THE ART	3
2.1	Operational Evaluation of Decelerators	6
2.1.1	Deployment	6
2.1.2	Inflation and Deceleration	10
2.1.3	Steady Descent	11
2.1.4	Termination	12
2.1.5	Typical Malfunctions	12
2.2	Design Considerations	13
2.2.1	Parachute-Design Parameters	13
2.2.1.1	Porosity	14
2.2.1.2	Shape	14
2.2.1.3	Unit-Canopy Loading	14
2.2.1.4	System-Mass Ratio	16
2.2.1.5	Trailing Distance	17
2.2.1.6	Scale Effects	18
2.2.2	Aerodynamic Characteristics of Deployable Wings	18
2.2.3	Performance of Supersonic Decelerators	18
2.2.4	Reefing-Design Parameters	21
2.2.5	Weight and Packaging	21
2.2.6	Ejection, Deployment, and Inflation Control Devices	23
2.2.7	Sensors and Controls	25
2.2.8	Materials	25
2.2.9	Fabrication Processes	27
2.2.10	Advanced Decelerator-Design Problems	29
2.3	Selection Procedures	31
2.4	Calculation of Design Loads and Stresses	31
2.4.1	Prediction of Opening Loads	32
2.4.2	Stress Analysis	32
2.5	Tests	33
2.5.1	Systems and Components	34
2.5.2	Materials	35
2.5.3	Joints, Seams, and Reinforcements	36

3. CRITERIA	36
3.1 Functional Considerations	36
3.2 Design Characteristics	37
3.3 Operational Conditions	38
3.4 Design Constraints	38
3.5 Selection	39
3.6 Design Analysis	39
3.7 Tests	41
4. RECOMMENDED PRACTICES	41
4.1 Functional Considerations	42
4.1.1 Deployment and Inflation	42
4.1.2 Deceleration	43
4.1.3 Stabilization	43
4.1.4 Steady Descent	43
4.1.5 Response to Control Signals	44
4.1.6 Aerial-Recovery Engagement and Towing	44
4.1.7 Terminal Deceleration and Touchdown	44
4.1.8 Termination	44
4.2 Design Characteristics	45
4.3 Operational Conditions	48
4.4 Design Constraints	49
4.5 Selection	52
4.6 Design Analysis	57
4.6.1 Decelerator Aerodynamic Performance	57
4.6.2 Opening Loads	59
4.6.3 Deployment (Snatch) Forces and Reaction Loads	60
4.6.4 Stress Analysis	61
4.6.5 Structural Design Factors	62
4.6.6 Deceleration Staging	64
4.6.7 Aerodynamic Stability	64
4.6.8 Wake Effects	64
4.6.9 Dynamic-Heating Effects	65
4.6.10 Aerodynamic Performance of Deployable Wings	65
4.6.11 Reliability	65
4.7 Tests	65
REFERENCES	69
SYMBOLS	77
NASA SPACE VEHICLE DESIGN CRITERIA MONOGRAPHS ISSUED TO DATE	81

DEPLOYABLE AERODYNAMIC DECELERATION SYSTEMS

1. INTRODUCTION

When a spacecraft mission includes entry into and descent through a planetary atmosphere of sensible density, a deployable aerodynamic deceleration system may be employed to control the spacecraft's motion in preparation for landing, aerial recovery, or initiation of other means (e.g., retrorockets) of effecting a terminal landing operation.

A typical deployable aerodynamic deceleration system is a combination of pliant fabric surfaces in the form of drogues, inflatable envelopes, and parachute-like devices, designed to decelerate, stabilize, and control the descent of the spacecraft. This type of system can produce large drag (or lift) surfaces from relatively small masses of material. These surfaces can be deployed in a series of incremental stages as an effective means of limiting peak loads, impact shocks, and decelerations imposed on the spacecraft and its cargo. During deployment, structural stresses on both the spacecraft and the decelerator are caused primarily from inertial and friction forces, and, during inflation, from aerodynamic forces generated by the transfer of kinetic energy from the entering spacecraft to the surrounding air.

The operational reliability of parachute landing systems has been extremely high. The only known catastrophic failure of a manned-spacecraft parachute system occurred with Russia's Soyuz 1 in April 1967 and cost the life of Cosmonaut Vladimir Komarov. It was learned that the main parachute system did not function properly and was not disconnected when Komarov deployed his reserve system. The reserve parachutes became twisted around the primary system and could not inflate. Deployable deceleration system failures, caused by design deficiencies and difficulties in adequately simulating operational conditions, have also been encountered during development tests.

Deployable decelerators are inherently structural systems. Surfaces, lines, and fittings are load-bearing extensions of the spacecraft. The storage, deployment, control, and release of the decelerator must be intimately integrated with the basic configuration to achieve overall flightworthiness. It is essential that this integration process begin early in the design phase.

Decelerators vary in their structural characteristics, flexibility of installation, deployability, reliability, and installed weight. Some decelerators have been developed to a high degree of usefulness; others are still experimental. Some relatively new devices may afford better engineering solutions than do long-used devices. However, costly errors have resulted from the selection of a partially developed component of a deployable deceleration system on the premise that the required performance could be delivered at the appointed time. A more common error is that of making insufficient allowance for spacecraft weight increase that inevitably occurs after the deployable deceleration system design has been frozen.

The history of the Apollo command module affords a dramatic example of the growth in payload weight during the course of design. Preliminary design allowed for a weight of 3860 kg (8500 lb). In the course of the program, however, the design weight grew incrementally to 5890 kg (13 000 lb), with no increase in allowable parachute size and an actual decrease in allowable parachute volume. The consequences were undesirable increases in the design terminal rate of descent and the need to provide for high-density pressure packing of the main parachutes.

This monograph provides criteria and recommends practices for the selection, design, analysis, and testing of deployable aerodynamic deceleration systems. It treats deployable devices of all types, along with their usage over a wide range of environmental and operational conditions; it also touches on the principal design factors relating to textile materials, dimensional stability, and fabrication processes. Primary emphasis is given to the various types of parachutes, deployable wings, inflatable envelopes, and attached or towed surfaces on which the most experience has been accumulated. These are most likely to be used on upcoming programs and therefore are of immediate interest to spacecraft designers. Lifting balloons and autorotors are accorded shorter treatment.

The size and required strength of the decelerator drag or lifting surface are determined by the spacecraft's gross weight and allowable load factor, and the velocity desired at the end of a deceleration stage or during steady descent. The flight conditions at deployment (altitude, velocity, and path angle) must be known, along with the density/altitude profile, to determine the type, number, and staging sequence of deceleration-system components; also the spacecraft's trajectory prior to the controlled-descent phase must be known. The aerodynamic characteristics of the main-descent surface are defined by the stability, controllability, and maneuverability required during the descent. For systems to be deployed in the atmospheres of planets other than the earth, environmental data needed for design include information on the composition and the density/altitude profile of the atmosphere and on surface gravity. Special design consideration must be given to scale effects, clustering effects, attached pilot-chute dynamics, dimensional stability, and unusual environments.

Other monographs which treat directly related subjects include those on entry thermal protection, landing impact attenuation for non-surface-planing landers, design-development testing, qualification testing, acceptance testing, and compartment venting. In addition, a monograph is in preparation on gasdynamic heating.

2. STATE OF THE ART

The technology of deployable aerodynamic deceleration systems advanced rapidly during the 1960's because of the impetus of intensive development programs carried out concurrently with spacecraft design, construction, and testing.

Heretofore, all operational spacecraft landing and recovery systems have been ballistic (i.e., drag-surface) decelerator systems. For the most part, these systems employ a drogue initial stage and a main descent-parachute final stage (e.g., the Mercury, Gemini, Apollo, Discoverer, PRIME, and ASSET systems).

The deployable aerodynamic deceleration systems developed for spacecraft have been primary landing or recovery systems (ref. 1), together with manned-spacecraft backup systems such as the Mercury reserve system (ref. 2) and the Gemini crew-escape system. Entry-capsule recovery systems have employed single and tandem parachutes designed in most instances for aerial pickup of the descending payload by loitering recovery aircraft, but also for lowering a space capsule to a soft landing (refs. 3 to 6). In all of these systems, the operational concept called for water landing as the primary mode, and design descent rates were generally too high for safe landing on dry ground.

Development of a lifting-surface decelerator (i.e., the paraglider) as a deployable land-landing system during an early stage of the Gemini program was eventually abandoned in favor of a more conventional ballistic system. A comprehensive technology-development program was also completed to establish the feasibility of a land-landing system for Gemini, employing a steerable parachute of L/D (lift-to-drag ratio) ≥ 1 , along with the retrorockets for terminal vertical velocity attenuation and extendable skids for impact attenuation.

Both ballistic- and lifting-flight concepts are currently being developed for new deployable deceleration systems. Probably the simplest of the new systems is the single circular parachute proposed for the Viking Mars lander. This parachute provides a transitional deceleration stage between the fixed-structure ("aeroshell") entry decelerator and the retrorocket landing system. A towed balloon-type decelerator has been proposed for a Venus lander.

By 1969, development of various deployable wing systems was being accelerated so that one or more of these systems may become operational in the 1970's. This development is directed toward steerable land-landing systems for projected advanced

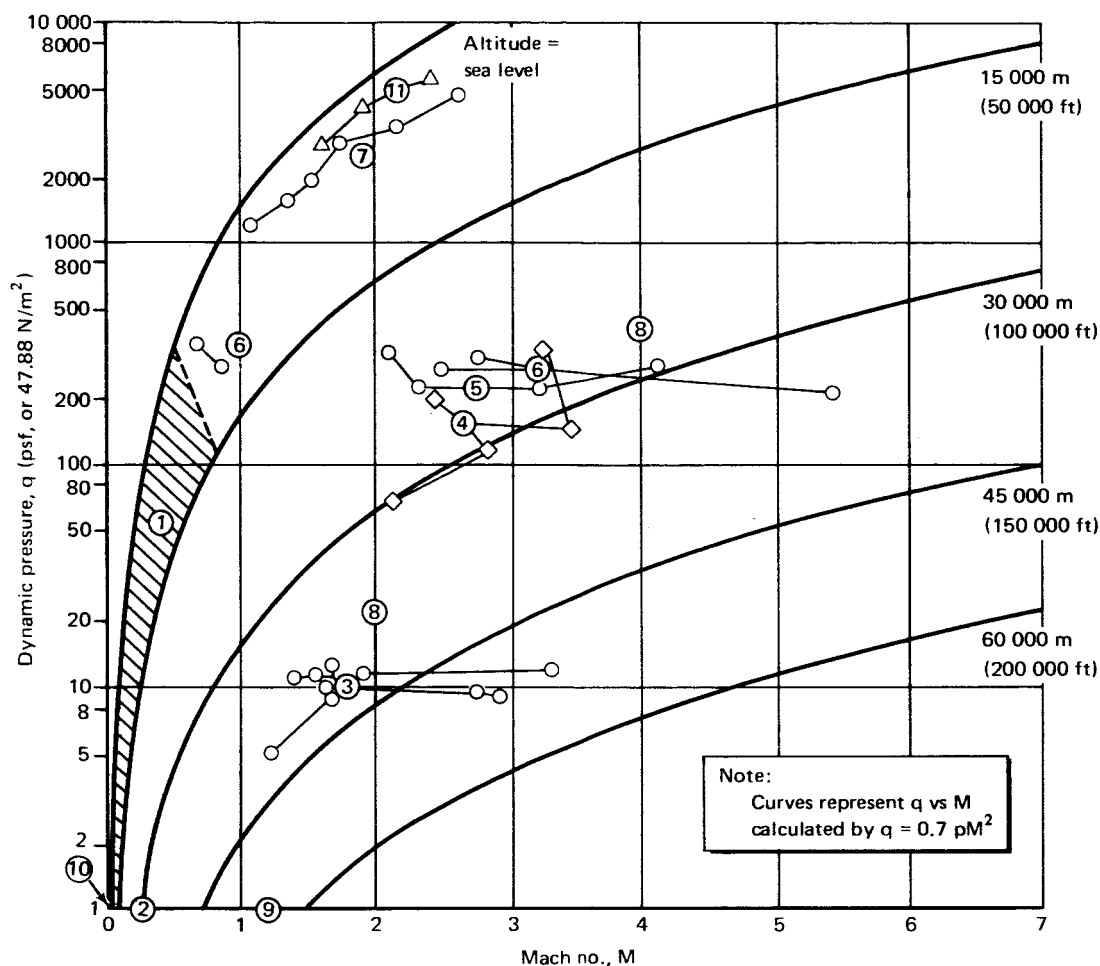
spacecraft of various configurations. These wing systems range from large ballistic-type capsules to lifting bodies of advanced design. Proposed backup or reserve landing systems for deployable-wing craft include both conventional parachutes and duplicate deployable-wing systems. A winglike surface poses a more difficult deployment problem than does either the ballistic or the steerable parachute. Deployment approaches being used successfully in current development programs include multistage lobe-by-lobe reefing and transferable-harness arrangements, along with pilot chutes and preceding drogue stages.

Reference 7, known popularly as the "Air Force Parachute Handbook," provides a comprehensive and detailed view of the state of the art in deployable aerodynamic decelerators in the early 1960's. Subsequent advances are presented by a rather voluminous literature (e.g., refs. 8 to 11), relevant portions of which are digested in this monograph.

Figure 1 illustrates the scope of test experience with parachutes, ballutes, and other decelerators in terms of altitude, dynamic pressure, and Mach number at deployment. The range of decelerator sizes tested is also indicated. A guide to symbols is presented at the end of the monograph.

The load-carrying capacity of aerodynamic deceleration systems is not a limiting factor in spacecraft applications. The practicability of handling suspended weights of up to 9072 kg (20 000 lb) with single parachutes approximately 57.91 m (190 ft) in diameter has been demonstrated, and monolithic vehicles weighing up to 20 700 kg (45 800 lb) have been air-dropped with heavy-duty ribbon parachutes (ref. 12). Deployable wing systems have been flown with a load of 2722 kg (6000 lb) (refs. 13 and 14). Single-ribbon drogues have been built to withstand ultimate loads of 1.334 MN (300 000 lbf), and successful operation after being subjected to opening loads of over 675 kN (152 000 lbf) has been demonstrated (ref. 15). Decelerator deployment at hypersonic speeds is feasible, but much testing remains to be done. A heat-resistant ballute has been deployed at a velocity approaching Mach 10 (ref. 16).

Considerable thought and effort have been directed toward determining the potential utility of decelerators other than that as parachutes, ballutes, and deployable wings. Some progress is being made in the development of attached inflatable decelerator designs (refs. 8 and 17). Autorotors have been developed for recovery of small payloads (refs. 7 and 18), while more advanced applications for various types of folding, telescoping, or stowable blades exist only as concepts on which preliminary design analyses have been performed (refs. 19 to 21). Similarly, concepts of hot-air balloons and other aerostat types (e.g., the "Paravulcoon") have been developed in considerable detail for booster-recovery applications (ref. 22); a practical demonstration of a hot-air balloon system was performed for the U. S. Air Force under the PARD program. Crew-escape systems envisioned for future use are treated in reference 23.



Group	Decelerator type	Size (diameter)
①	Conventional parachutes Gliding parachutes Deployable wings Aerial-recovery parachutes	$D_p = 0.3-61$ m (1-200 ft) $D_o = 4.9-27$ m (16-88 ft) $b_w = 3.7-27.4$ m (12-90 ft) $D_o = 7.3-21.4$ m (24-70 ft)
②	Sounding-rocket parachutes	$D_o = 1.8-4.9$ m (6-16 ft)
③	Planetary-entry parachutes	$D_o = 4.1-26$ m (30-85 ft)
④	Experimental hemisflo and hyperflo drogues	$D_o = 0.82-1.98$ m (2.7-6.5 ft)
⑤	Experimental textile ballutes	$D_p = 0.61-1.52$ m (2-5 ft)
⑥	Experimental parasonic drogues	$D_o = 1.22$ m (4 ft)
⑦	Hemisflo drogues	$D_o = 4.88$ m (16 ft)
⑧	ALARR ballutes	$D_p = 0.61$ m (2 ft)
⑨	Sounding-rocket ballutes	$D_p = 2.13-4.88$ m (7-16 ft)
⑩	Experimental AIDs	$D_p = 11.28$ m (37 ft)
⑪	Conical-ribbon parachutes	$D = 3.81-23.2$ m (12.5-76 ft)

Figure 1. — Decelerator flight-test experience.

Table I presents a summary of descriptions, general-performance characteristics, and the development status of most of the known deployable aerodynamic decelerators. Those classed as "operational" performed successfully in operational systems, and adequate design data are available. "Advanced" decelerators have had limited operational use but have undergone extensive testing (including flight testing) in development programs. "Obsolescent" decelerators are candidates for replacement with advanced models. Decelerators classed as "experimental" either have not been subjected to sufficient full-scale flight testing or still have unsolved operational problems. The decelerators classed as "conceptual" are those whose designs appear to be based on demonstrated physical principles rather than prototype tests. Engineering data on performance characteristics, functional limitations, and model-scaling laws for all types of decelerators are generally incomplete; these shortcomings constitute major design problems that must be faced in new programs.

2.1 Operational Evaluation of Decelerators

The most useful characteristic of a deployable aerodynamic deceleration system is its ability to produce a relatively large drag or lifting surface from a small mass of material (typically 3 to 7 percent of the vehicle mass). Moreover, these systems can be packaged and stowed in any convenient compartment or in an odd-shaped residual space in a vehicle.

There are several functional phases of deployable decelerators which must be achieved in sequence. These are:

- Deployment
- Inflation and deceleration
- Steady descent
- Termination

In each case, the preceding phase must be properly completed before the next can begin. General requirements for each of these functional phases must be satisfied more or less independently to ensure the flightworthiness of the system as a whole.

2.1.1 Deployment

The first phase of decelerator operation is *deployment*. Specifically, it is the process of ejecting or extending the decelerator from its compartment into the airstream until it is fully stretched out and ready to inflate.

A deployment bag is used to provide a container for packing all types of towed decelerators. Retainers for risers, lines, and canopy in the deployment bag provide for

TABLE I. — DEPLOYABLE AERODYNAMIC DECELERATORS

Class and type	Description	General performance (a)	Development status	Source of design data (ref. no.'s)
PARACHUTES				
<u>Drogue or pilot</u>				
Guide surface	Flat crown; conical skirts; canopy with or without ribs.	Stable subsonic drogue; medium shock; low C_{D_0} .	Operational (subsonic)	7
Conical ribbon	Ventilated ribbon canopy.	Stable drogue to Mach 1.5; low shock; medium C_{D_0} .	Operational	1,7, 24
Hemisflo	Hemispherical; extended skirt-ribbon canopy.	Stable drogue to Mach 2.5-3; low shock; low C_{D_0} .	Operational	7,15,24,25, 26
Hyperflo	Flat porous crown; conical skirt.	Tested as supersonic drogue to Mach 4; erratic C_{D_0} .	Experimental	15,24,26,27, 28
Parasonic	Improved version of hyperflo with analytically shaped canopy.	Stable supersonic drogue tested to Mach 5.5; medium shock; low C_{D_0} .	Experimental	15,16,27,29 30
Vane	Hemispherical canopy with or without deployment spring.	Stable pilot chute; low C_{D_0} .	Operational (subsonic)	7
<u>Main descent</u>				
Flat circular	Classical parachute prototype, solid cloth; regular polygon	Unstable; large oscillations; high shock; high C_{D_0} .	Operational	7,31,32
Extended skirt	Solid cloth; extended shaped skirt.	Large-scale models have low shock, medium stability, high C_{D_0} .	Operational	7,31,33
Bi-conical, tri-conical	Solid cloth; bi- or tri-conical skirt.	Large-scale models have low shock, medium stability, high C_{D_0} .	Operational	7,32,33
Ringsail	Annulate, ventilated, ogival canopy.	Large-scale models have medium shock, medium stability, high C_{D_0} .	Operational	7,34,35,36
Ringslot	Annulate, ventilated, flat, circular canopy.	Low shock; stable; medium C_{D_0} .	Operational	1,7
Disk-gap-band	Canopy ventilated with wide peripheral slot; flat crown; cylindrical skirt.	Medium shock; medium stability; medium C_{D_0} .	Advanced	11
Annular	Truncated toroid, solid-cloth canopy with internal lines.	Medium shock; good stability; high C_{D_0} .	Advanced	3,4
Cross	Cruciform, flat canopy.	Medium shock; good stability; high C_{D_0} .	Advanced (subsonic)	37

^aSee Symbols list for definitions.

TABLE 1. – DEPLOYABLE AERODYNAMIC DECELERATORS – Continued

Class and type	Description	General performance (a)	Development status	Source of design data (ref. no.'s)
PARACHUTES (Continued)				
<u>Steerable</u>				
Glidesail	Steerable version of ringsail, using standard parachute cloth.	Low shock; low L/D max.	Advanced	
Parasail	Complex ventilated canopy of low-porosity cloth.	Medium shock; low L/D max.	Operational	38, 39
Cloverleaf	Fused cluster of three circular sailcloth canopies.	High shock; medium L/D max.	Advanced	40
<u>Aerial Recovery</u>				
Tandem canopy	Ringslot target, trailing ringsail man on long tow line.	Low shock; poor target stability; low C_{DS}/W_p .	Obsolescent	3
Conical extension	Conical frustum target on extended skirt canopy.	High shock; good stability; deployability under development.	Advanced	3, 5, 6
Ringsail/annular	Ringsail target close-coupled above annular main.	Medium shock; good stability; high C_{D_o} ; medium C_{DS}/W_p .	Advanced	3, 4
<u>Rotating</u>				
Vortex ring	Complex, free-fabric windmill with four vanes; swivel required.	Low shock; good stability; high C_{D_o} ; high C_{DS}/W_p .	Operational	7
Rotafoil	Ventilated circular canopy with radial slots; swivel required.	Low shock; good stability; high C_{D_o} ; medium C_{DS}/W_p .	Operational (subsonic)	7
DEPLOYABLE WINGS				
Parawing	Truncated triangular planform; one or two keels; deflected tips.	Operational performance expected from deployable-wing group –	Advanced	13, 14, 41, 42, 43
Sailwing	Rectangular planform; two or three keels; deflected triangular tips.	L/D max: 1.5-3 L/D modulation: 1.0–L/D max Turning rate: 5–25 deg/sec	Advanced	44
Parafoil	Rectangular planform; ribbed double surface; ram-inflated cells.	Touchdown: flared landing.	Advanced	45, 46
Volplane	Modified version of parafoil with single surface aft of mid-chord.		Advanced	Pioneer Parachute Co. data sheets.

^aSee Symbols list for definitions.

TABLE I. — DEPLOYABLE AERODYNAMIC DECELERATORS — Concluded

Class and type	Description	General performance (a)	Development status	Source of design data (ref. no.'s)
INFLATABLES				
<u>Towed</u>				
Ballute	Isotenoid envelope; ram-air (water-alcohol) inflated.	Hypersonic drogue tested to Mach 9.7; low shock; stable.	Operational	7, 15, 27, 30, 31, 47
Balloon	Spherical envelope; ram-air or gas pressurized.	Low shock; unstable.	Experimental	7, 48, 49
Cone	Conical envelope; ram-air or gas pressurized.	Low shock; stable.	Experimental	7, 48
<u>Attached</u>				
Isotenoid envelopes (AID's)	Base-mounted; ram-air or gas pressurized.	Low shock; stable.	Experimental	8, 17, 50
Airmat cone	Base-mounted, double-walled, conical envelope; gas pressurized.	Low shock; stable.	Experimental	
AUTOROTORS				
Flexible blade	Blades of coated fabric that can be rolled to hub for stowage.	Operational performance of successful autorotors is expected to be equivalent to that of deployable wings.	Experimental	7
Folding blade	Articulated rigid blades stowable by folding up (or aft) from hub.		Experimental (small scale)	7, 21
Telescoping blade	Articulated rigid tubular blades with telescoping segments.		Conceptual	19, 21
Inflatable blade	Gas-pressurized blades of coated fabric, deflated and rolled for stowage.		Conceptual	21
MISCELLANEOUS				
Flexible brake	Body-mounted folding arms with fabric panels between.	Low shock; stable.	Experimental	51

^aSee Symbols list for definitions.

the escape of only one canopy segment at a time as the bag moves aft in the air stream. This ensures that stretchout of risers, lines, and canopy will be orderly, and that the initial drag area presented to the airstream by the deploying system will be a minimum. The small drag area exposed during deployment reduces the relative acceleration of pack and vehicle, and thereby minimizes the impact load applied to both when the lines become taut. Shock-attenuating riser assemblies also are used to reduce impact loads.

The mortar is commonly used for ejecting a decelerator pack forcibly into the airstream; various types of slug guns, thrusters, and catapults are also available for this purpose. Decelerator packs weighing up to approximately 56.7 kg (125 lb) have been deployed successfully from mortars. A 49-kg (108-lb) pack catapult has also had operational use (ref. 52).

2.1.2 Inflation and Deceleration

The second phase of decelerator operation, *inflation and deceleration*, can be controlled in varying degrees to limit impact shocks. A high degree of control can be obtained with attached inflatables, and a partial degree of control with towed decelerators.

Controlled growth of decelerator area to limit peak loads and decelerations has usually been accomplished on operational spacecraft by both (1) successive deployment of separate decelerators of increasing area as the dynamic pressure diminishes, and (2) restricting the initial area of an individual decelerator while the dynamic pressure is high, then increasing the area either continuously or in steps as the dynamic pressure diminishes. The typical deceleration system employs one drogue and one main-descent surface in which the drogue may have one reefed stage and the main surface may have one, two, or more reefed stages. A draw-string or reefing line around the mouth of the canopy restricts area growth temporarily. A step-area increase occurs when the reefing line is severed by a pyrotechnic cutter after a predetermined delay. Since all conventional reefing-line cutters are initiated by a lanyard at line stretch, additional step-area increases are obtained with successively longer built-in time delays in each set of cutters.

Continuously variable reefing controls for parachutes have not been developed to a practical level. The main problem is reliability; i.e., ensuring an acceptably high probability that no possible malfunction could prevent completion of area growth.

In autorotor deployment, the major reliability problem has been how to ensure synchronous extension of all blades prior to and during spin-up, a problem which may account for the fact that only small-scale deployable autorotor systems have been successful.

2.1.3 Steady Descent

The third phase of decelerator operation, *steady descent* at near-equilibrium velocity, can be achieved when one of the decelerators is retained in an operational stage for longer than a few seconds, or long enough for the flight path to approach the vertical. Present theory of decelerator motion during steady descent is summarized as follows:

- System oscillation is caused by lift or transverse forces that develop in various ways, such as through periodic vortex-shedding from the drag surface.
- When the vortices form and shed alternately from side to side, a fairly regular transverse oscillation results; at other times, coning oscillations may be experienced.
- If there is a dissymmetry in the drag surface (placed there either by design or accidental damage) that causes vortex formation in a fixed pattern, a stable glide with very little oscillation will be produced. Steerable parachute designs are based on this phenomenon.

Steady descent of the system with the main-decelerator surface is attended by drift with the wind and by random augmentation of normal oscillations by wind-shear strata and gusts. Damping of imposed oscillations of greater than normal amplitude is generally completed within one full cycle, the damping interval being somewhat shorter for steerable parachutes than for polysymmetric parachutes. A cluster of parachutes shows better stability than its individual members, and large parachutes are generally more stable than small models of the same type. A steerable parachute or a deployable wing is exceptionally stable and has good damping characteristics when gliding within its normal L/D range. Operation at low L/D may be attended by parachute-like oscillations. At high L/D the leading edge may collapse, followed by large-amplitude oscillations, until corrected by a pitch-control adjustment (refs. 41, 45, and 53).

During turning maneuvers, the sinking speed of a gliding system increases in proportion to the rate of turn. The sinking speed also increases with a controlled reduction in L/D and during a stall, but lift recovery is rapid when the gliding surface is trimmed. With some deployable-wing systems, it is possible to perform a terminal flare maneuver to reduce the touchdown velocity (ref. 45). The horizontal-velocity component enables wing penetration of winds of 9.1 to 18.3 m/sec (30 to 60 fps) depending upon the maximum L/D of the deployable wing and the sinking speed of the system.

Reduction of sinking speed to zero at a predetermined altitude is considered feasible by at least two methods, neither of which has been demonstrated with a deployable deceleration system of the efficiency required for spacecraft recovery. One method uses an aerostat or lifting balloon; the other requires the propelling or towing of a

deployable-wing system. To enable the vehicle to be flown to a favorable landing site, short-range propulsion by rocket or turbojet has been proposed. This conceptual mode of operation may be considered somewhat beyond the present state of the art in deployable-wing systems, as are conceptual autorotor systems; however, engine-propeller-powered flight has been demonstrated (ref. 45).

2.1.4 Termination

Termination of operation of the deployable deceleration system is effected in different ways for different purposes. When the collapse of the system after landing cannot be ensured because of surface winds, the main surface is designed to disconnect from the vehicle (refs. 7 and 54). An automatic disconnect of the main decelerator may be actuated at a predetermined altitude by a signal which initiates the firing of a retrorocket landing system, as planned for the Viking Mars lander. Parachute operation in an aerial-recovery system is terminated when the canopy is collapsed by the pickup system during the mid-air engagement; otherwise, operation continues to a normal landing on the surface.

2.1.5 Typical Malfunctions

Failures of deployable deceleration systems have generally occurred during development-test programs because of errors in establishing the test conditions or because of design deficiencies. Following is a discussion of the various types of malfunctions that have been experienced prior to qualification of the operational landing or recovery system:

- Deployment malfunctions – caused by obstructions in the deployment path; inadequate allowance for vehicle spin or tumbling; improper angle of ejection, insufficient ejection energy; inadequate reliability of initiators; improper packing and/or rigging; unforeseen environmental factors; and impact-shock waves in the towing riser.
- Inflation and deceleration malfunctions – caused by insufficient structural strength, premature deployment; deployment malfunction; riser abrasion, notching, or cutting; insufficient allowance for vehicle spin; insufficient allowance for vehicle-wake effects; insufficient allowance for nonuniform loading; excessive porosity; neglected operational variations; reefing-line-cutter failure; premature separation of reefing line; premature separation of a prior-stage decelerator; malfunction of a prior-stage decelerator; and undamped high-frequency oscillations.
- Descent malfunctions – caused by major damage to the primary drag or lifting surface; distortion of the primary drag or lifting surface by fouled rigging; interference between clustered canopies; impact of a previously

jettisoned spacecraft component; excessive undamped oscillations; excessive relative motion between primary lifting surface and suspended vehicle; fouled control lines; excessive porosity; and effects of dimensional instability on trim and control of lifting surface.

- Aerial recovery malfunctions – caused by deployment malfunction; collapse or inadequate stability of target canopy; and insufficient structural reinforcement of parachute assembly for engagement impact.

2.2 Design Considerations

The importance of weight in spacecraft design has placed special emphasis on the aspects of deployable deceleration systems that determine component and installed weights. Emphasis is directed at stowage requirements, control requirements, deployment characteristics, component strength, and the manner in which applied loads are absorbed and distributed in the decelerator and spacecraft. Accordingly, parachute efficiency is calculated as the ratio of its effective drag area to weight (C_{DS}/W_p). The drag/weight efficiency is one of the factors used in evaluating the suitability of different types of decelerators for a specific application.

Generally, the state of the art in decelerator design is limited by present understanding of the way in which the aerodynamic characteristics are determined by the mechanical and structural characteristics of the decelerator and of the mass dynamics of the vehicle-decelerator system.

The aerodynamic characteristics of all fabric decelerators are the product of shape and porosity factors that distinguish one type or class of fabric decelerator from another. Almost without exception, all towed and attached decelerators of the ballistic, or nongliding, type are symmetrical about the longitudinal axis. The planform of gliding parachutes is a planar-symmetric modification of either a circular shape or a fused cluster of circles. Deployable wings of interest are lobed or cellular surfaces approximating an ellipse or rectangle in planform, with aspect ratios greater than unity; they also have substantial lateral area in the form of keels, ribs, rigging flares, and deflected tips. Among the different types of decelerators, there is generally an underlying consistency in the design of features having similar aerodynamic or structural functions.

2.2.1 Parachute-Design Parameters

Typical relationships between various parachute-design parameters and aerodynamic-performance characteristics are illustrated schematically in figure 2. Although wind-tunnel tests have been used to determine force and moment coefficients for some types of parachutes, the preponderance of aerodynamic data available for design is from aerial-drop tests. Consequently, there is a notable lack of

data on tangent (C_T), normal (C_N), and moment (C_M) force coefficients and their derivatives for some of the most widely used parachute designs (e.g., ringsail).

2.2.1.1 Porosity

The total *porosity* (λ_T) of a parachute canopy includes both the minute interstices, or "pores," between the yarns of the woven fabric (fabric porosity), and the larger designed-in vents and slots (geometric porosity). As indicated in figure 2, the total porosity of the canopy (λ_T) strongly affects the drag coefficient, the filling time (represented by the dimensionless filling interval K_f), the opening shock (represented by the dimensionless opening-load factor C_K), and the static stability (slope of the pitching-moment curve with respect to θ) of the parachute system. A specific determination of the relationships between porosity and aerodynamic characteristics is dependent on the pattern of the distribution of the porosity across the canopy, and by the scale of the canopy.

In parachutes, porosity and the distribution of porosity across the canopy are major design parameters. Steerable parachutes perform adequately with canopies which are partially porous to limit opening-shock loads, but near-zero-porosity sailcloth is used in most steerable parachutes to maximize L/D. The other types of decelerators, such as ballutes, attached inflatable decelerators (AIDs), and deployable wings, also require fabrics of near-zero porosity for their proper functioning.

2.2.1.2 Shape

Parachute shape factors include the constructed profile (flat, conical, or spherical) and the planform (circular, square, triangular, or cruciform). In circular canopies, the most important shape factors are those which govern the angle of attack of the skirt (as seen in guide-surface, extended-skirt, and flared-skirt designs). For canopies with unconstrained skirts, the relative length of suspension lines (ℓ_s/D_0) is significant because it affects the inflated diameter of the parachute as well as the angle of attack of the skirt. All shape factors influence the aerodynamic characteristics of parachutes, and the effects can be determined by suitable experiments. Presently, only the effect of suspension-line length on drag coefficient is defined adequately in quantitative form for different types of parachutes (fig. 2b).

2.2.1.3 Unit-Canopy Loading

The *unit-canopy loading*, or ratio of the weight of the vehicle-decelerator system to the full-open drag area (W/C_{DS}), determines the equilibrium rate of the system's descent in still air. Changes in unit-canopy loading affect the operating characteristics of the parachute in ways that cause the drag coefficient to vary with rate of descent (fig. 2d). Below a unit-canopy loading of 24.0 N/m^2 (0.5 psf), oscillation or gliding of the parachute increases, causing the sinking speed to be lower than that of the

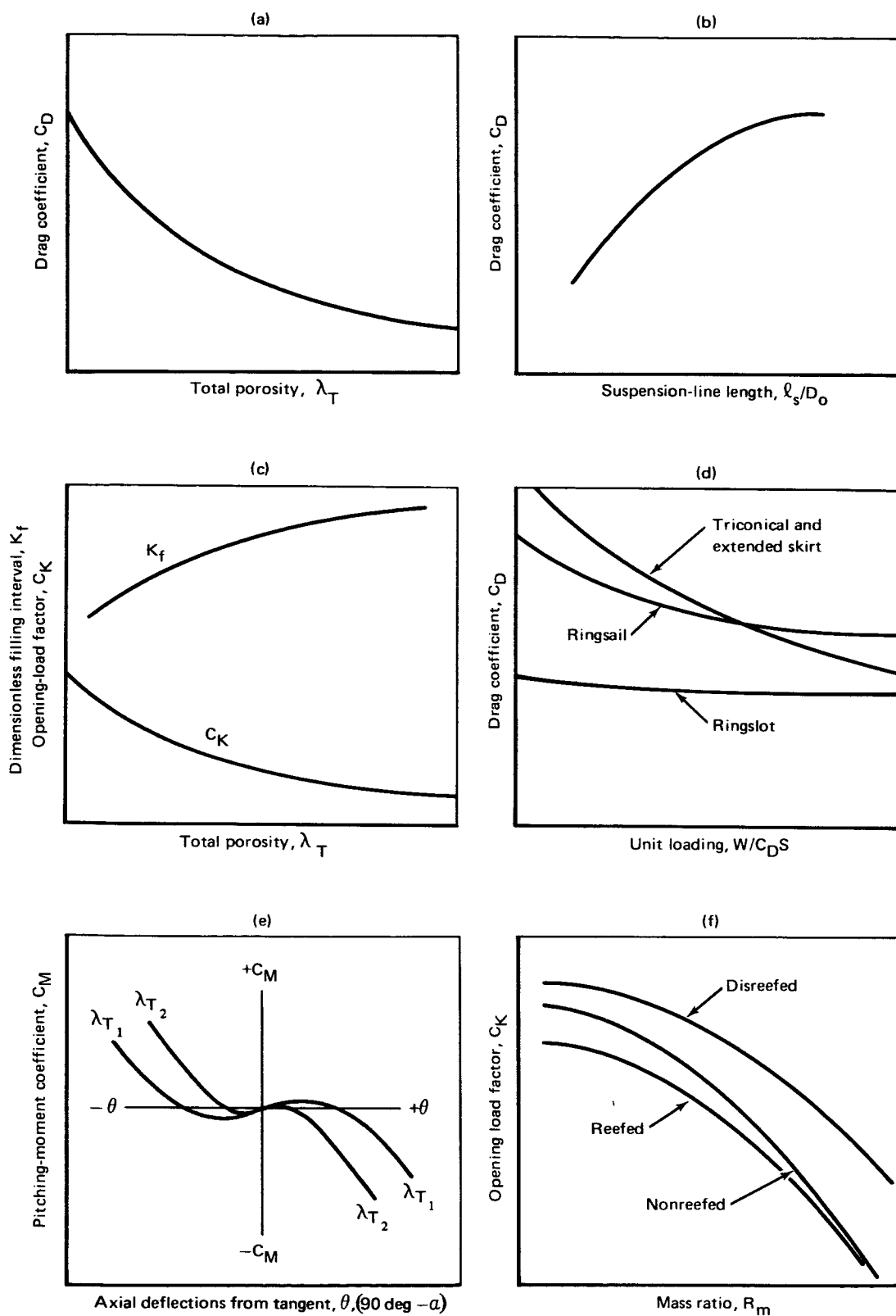


Figure 2. — Aerodynamic and design characteristics of parachutes.

nonoscillating system (i.e., the effective-drag coefficient is increased). With increased unit loading, an increase in rate of descent is attended by a higher differential pressure across the canopy which causes the relative porosity of the canopy to increase in proportion to its structural elasticity (fig. 3) (i.e., the effective-drag coefficient is decreased).

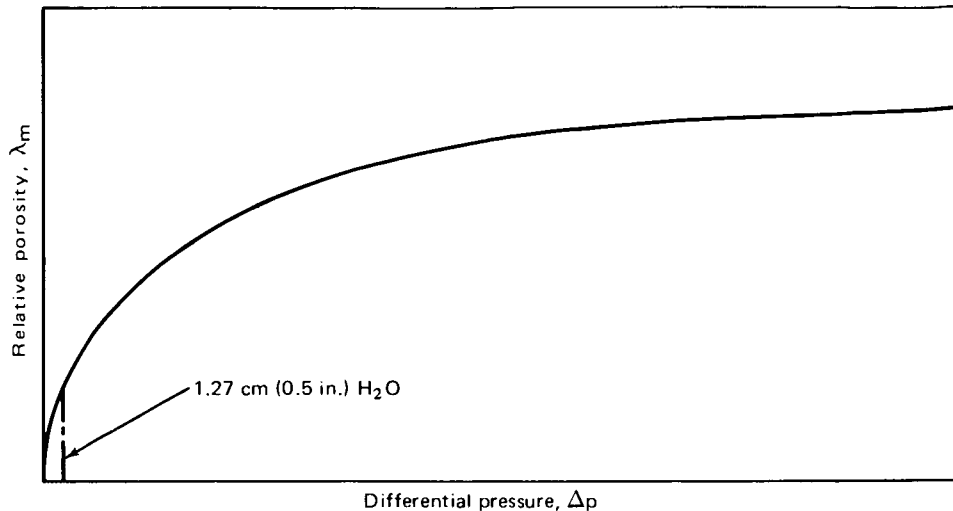


Figure 3. — Effect of differential pressure on relative porosity of parachute cloth.

This behavior places an upper limit on unit-canopy loading for certain types of solid-cloth canopies. The limit is reached when the relative porosity increases to the point where the ratio of inflow to outflow comes to equilibrium before the canopy is fully expanded, and so-called “squidding” takes place. Solid-cloth canopies with inverted-conical skirts are subject to this loading limitation, while circular flat and conical canopies are not. Canopies of annulate construction, such as the ringslot and ringsail types, have a smaller total variation of drag coefficient with unit loading.

The decline of drag coefficient with increased unit loading of solid-cloth canopies may be corrected by employing nonstandard fabric of low porosity, but the resulting augmentation of both instability and opening shock has created formidable development problems, such as the need for developing multistage-reefing techniques.

2.2.1.4 System-Mass Ratio

Theory supported by test results shows that the opening shock of a parachute is proportional to the *mass ratio* (ratio of the mass of air moving with the canopy to the mass of the vehicle plus parachute) and to Froude number (ref. 55). Empirical data have been evaluated by defining the mass ratio as $R_m = \rho D_o^3 / M$ and representing the opening shock by the Euler number, defined as $E_n = F_o / q_1 S_o$, where F_o is the measured peak opening force. To make this approach applicable to reefed as well as to

nonreefed parachutes, the mass ratio is redefined here as $R_m = \rho \psi^{3/2}/M$, where $\psi = C_{DS}$, and the opening load factor $C_K = E_n/C_{D0}$ is substituted for Euler number. In the new definition, the characteristic diameter of the canopy is represented by the square root of the effective-drag area, $\psi^{1/2}$, either reefed or full open. The variation of the opening-load factor with mass ratio for reefed and nonreefed parachutes follows the general trends illustrated in figure 2f. This relationship is considered more dependable than long-used empirical formulas relating opening-shock factor, X (or opening-load factor C_K) and unit-canopy loading, W/C_{DS} , with dynamic pressure and altitude as the related independent variables. However, the great mass of empirical data in the form of C_K versus W/C_{DS} is still valid and useful within the speed and altitude ranges of the tests that generated the data.

2.2.1.5 Trailing Distance

Decelerator performance is degraded by the proximity and the size of the towing body. Typical degradation in subsonic decelerator drag caused by body wake is shown in figure 4 as a function of the relative trailing distance and the relative size of the decelerator. Supersonic decelerators exhibit similar behavior, but the effects tend to be more severe for high-drag bodies and for relatively small decelerators (refs. 7, 29, 56, and 57).

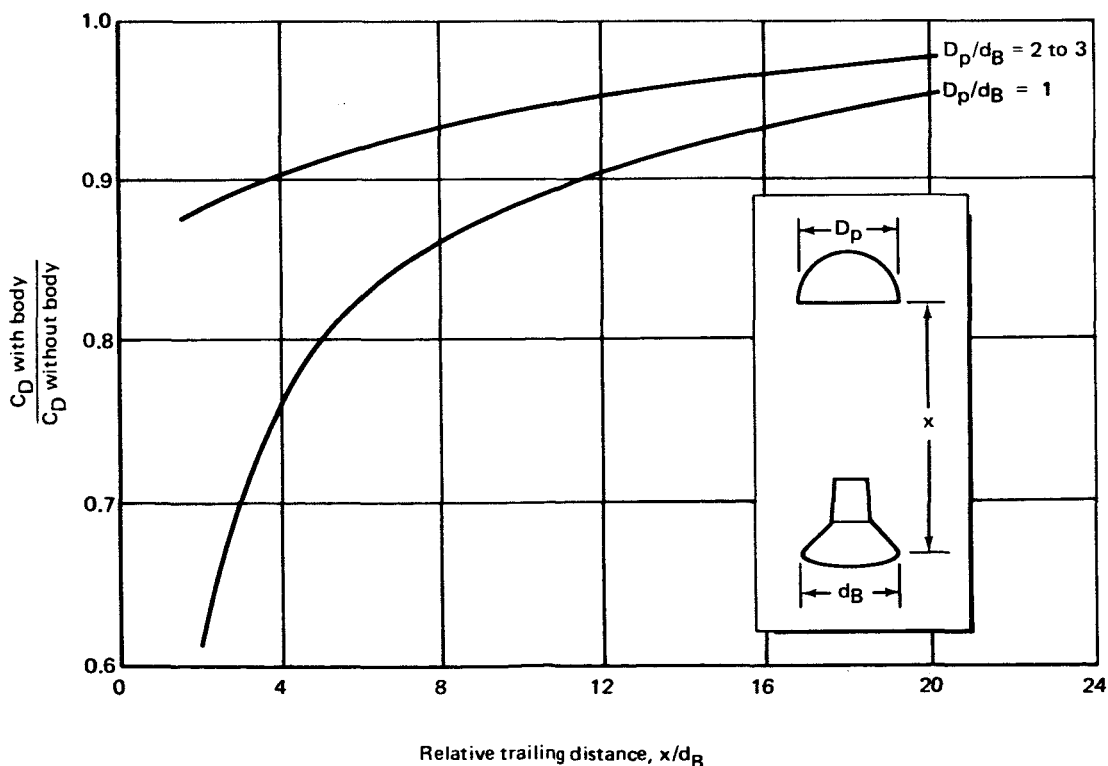


Figure 4. — Typical effect of trailing distance on decelerator-drag coefficient (subsonic).

2.2.1.6 Scale Effects

Parachute performance is affected markedly in various ways by changes in the absolute size, or "scale," of the canopy. These scale effects are numerous and complex, and are seldom clearly related to Reynolds number, probably because the ratio of fluid momentum to viscous forces described by Reynolds number includes a characteristic length which has uncertain meaning when applied to a parachute. Generally, the scale effects embody a combination of macroscopic and microscopic factors (for example, vortex formation and shedding combined with flow through the pores of the fabric). Other aspects of this subject are treated in the discussion of special problems associated with advanced decelerator design in Section 2.2.10 of this monograph.

2.2.2 Aerodynamic Characteristics of Deployable Wings

The design-relevant aerodynamic characteristics of deployable wings are illustrated schematically in figure 5. (The characteristics of steerable parachutes are similar.) The bulk of currently available performance data is limited to the results of wind-tunnel and free-flight tests of small-scale models with a lifting surface, S_w , of up to $\cong 16.2 \text{ m}^2$ (174 ft^2). With the exception of results of parawing tests, the results of intermediate-to large-scale tests of deployable wings have not been published. A comparison of large- and small-scale parawing free-flight performance is made in reference 13, and a structural-optimization study of large-scale parawings is reported in reference 58, which also discusses the aerodynamic characteristics of such decelerators, including the effects of reefing and porosity on opening loads.

Characteristically, the lift-to-drag ratio (L/D) of a deployable gliding surface can be controlled by varying the angle of attack, α , over a range of flight attitudes between leading-edge collapse and the stalling point (fig. 5a). The conventional pitch-control system changes the angle of attack by extending or lengthening lines attached to trailing-edge portions of the wing. Leading-edge collapse will occur at flight angles of attack, a little below the angle of attack for maximum L/D (fig. 5b). At the stalling point, lift falls off rapidly and the system usually becomes unstable, like a parachute of low porosity. Between the limits of leading-edge collapse and stall, oscillation damping is strong and gliding flight is quite stable (with the pitching-moment coefficient, C_M , varying almost linearly with angle of attack, as shown in fig. 5c). As the steering control deflection is increased, turn rate approaches an upper limit (fig. 5d); this limit decreases with increasing scale of the deployable wing. In flight, the vertical sinking speed is a minimum near L/D max (fig. 5f), and increases with controlling deflections that either reduce L/D or increase the turning rate. With a sufficient range of L/D modulation in stable flight, a pilot can execute a flared-landing maneuver with a deployable wing to reduce the touchdown velocity.

2.2.3 Performance of Supersonic Decelerators

A wide variety of deployable decelerators (usually called "drogues") have been developed for the purpose of augmenting the drag and stability of a descending vehicle.

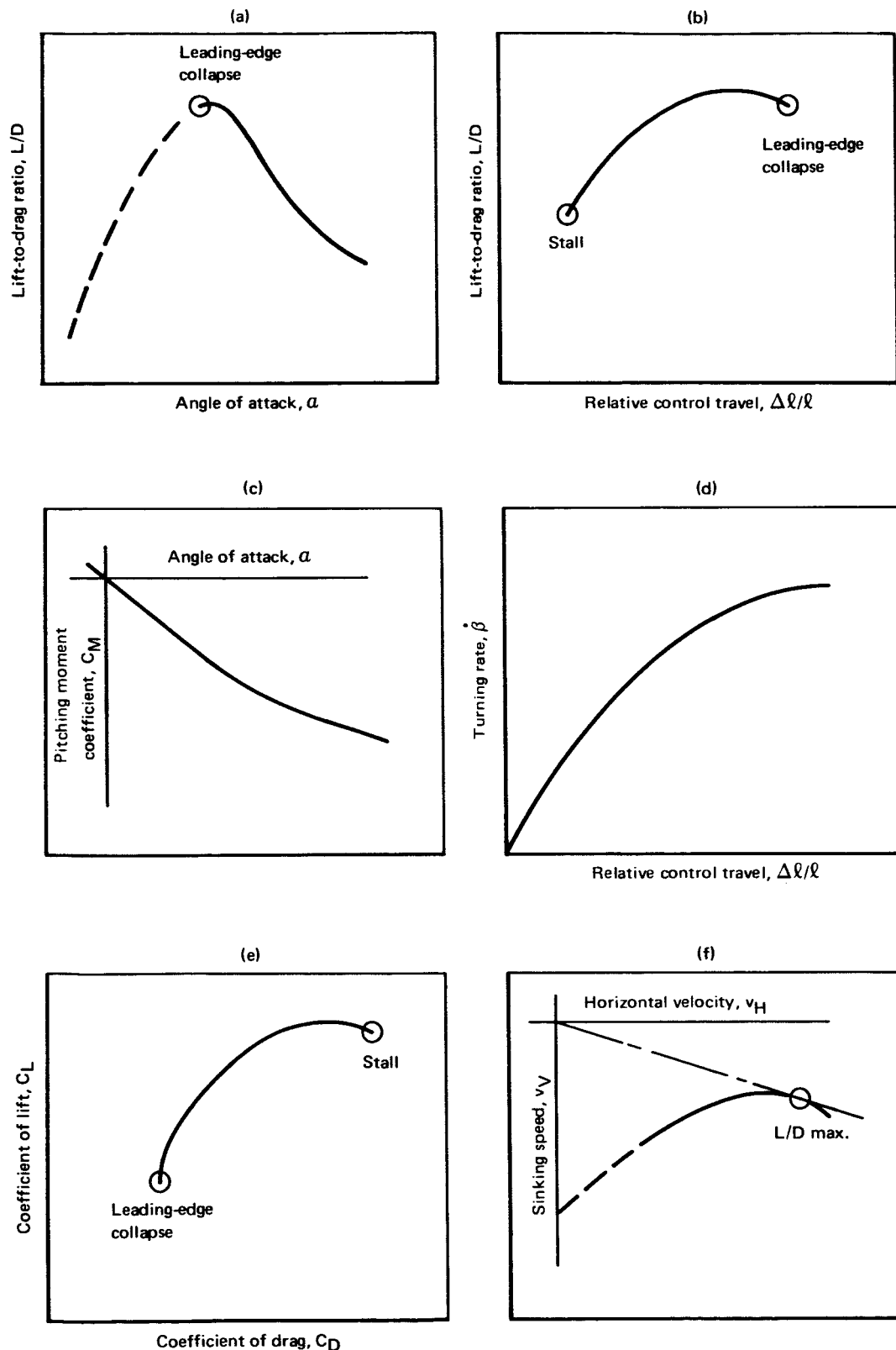


Figure 5. — Aerodynamic characteristics of deployable wings.

Of these, only a few perform well in supersonic flow. The most successful supersonic-drogue types are the conical-ribbon, hemisflo, and parasonic parachutes, and the ballute, a ram-air-inflated, quasi-isotensoid envelope. The parasonic design was derived from a somewhat less stable predecessor called the "hyperflo." Of the supersonic-drogue types, the conical ribbon has shown the best subsonic performance and, above Mach 1.5, the poorest supersonic performance.

The general decline in the drag coefficient of parachute drogues with increasing speed above Mach 0.8 (illustrated in fig. 6) is caused by a combination of wake effects and increasing-inflation instability. In the middynamic-pressure range (where most of the data have been obtained), inflation instability tends to limit the usefulness of a supersonic-drogue design to a velocity range somewhat below the maximum-test Mach number indicated for each type in figure 6. Inflation instability is characterized by alternate opening and squidding of the drogue canopy at high frequency and is attributed to periodic changes in the shock-flow pattern through and around the canopy, coupled with disturbances in the vehicle wake. The drag-coefficient data from which figure 6 was developed are from many sources (representing drogues tested in a variety of forebody wakes); these were reduced to a common base by using the total surface area of each drogue type as the reference area. Hyperflo-drogue data from tests at velocities up to Mach 4.1 were too scattered for meaningful presentation in this figure.

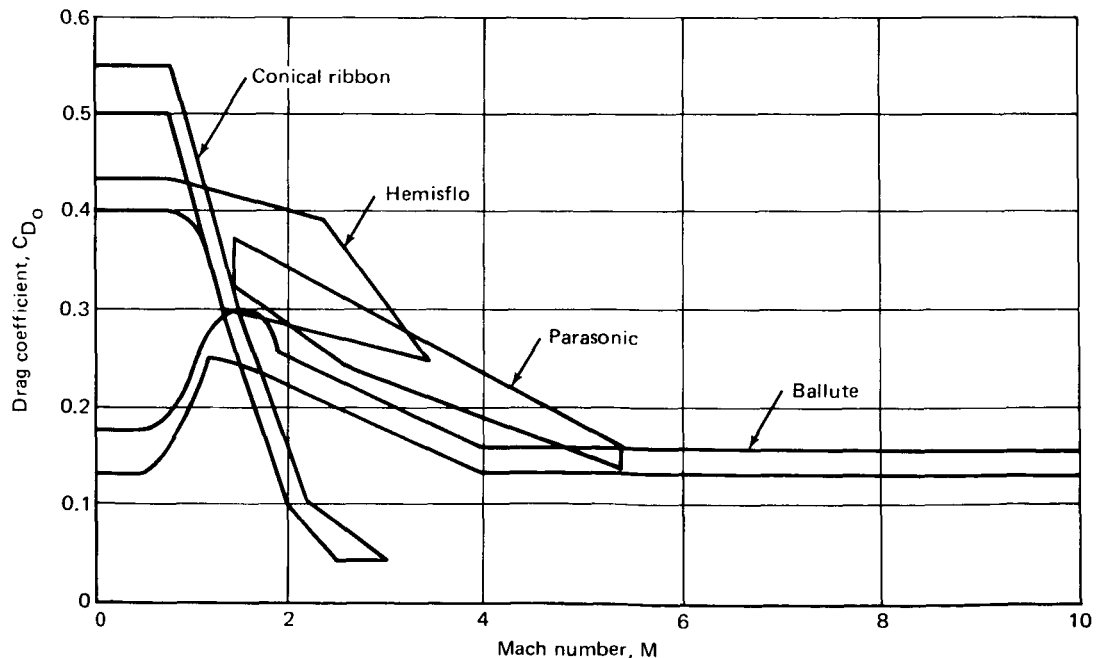


Figure 6. — Variation of drag coefficient with Mach number for various drogues.

The ballute drogue is an exceptionally stable, low-opening-shock device in the hypersonic speed range where the parachute drogues exhibit high-opening-shock

characteristics and increased inflation instability. Available ballute data are for models equal to or larger in diameter than the towing body; drogue-parachute data are for models equal to or larger than one-half the diameter of the towing body.

The effects of aerodynamic heating on supersonic decelerators are a function of true airspeed, dynamic pressure, and the duration of the heat pulse. Significant heating has been encountered in tests at Mach 3 to 6 in the dynamic-pressure regime of 4788 to 16 760 N/m² (100 to 350 psf). Protective coatings and Nomex textiles have been used to provide structures of strength adequate for the temperatures generated under these conditions (refs. 12, 15, and 16). However, measured temperatures in general have been much lower than predicted; for example, 367K (200°F) versus 427K to 538K (300°F to 500°F) predicted for a Nomex parasonic drogue deployed at Mach 5.4, and a dynamic pressure of 10 203 N/m² (213 psf) (ref. 16). All indications emphasize the practicability of using standard nylon textiles in supersonic decelerators for operation at speeds up to Mach 3. The feasibility of deploying large Dacron parachutes of relatively lightweight construction at Mach numbers on the order of 3 has been demonstrated at altitudes where dynamic pressures did not exceed 575 N/m² (12 psf) (ref. 11). Minor heat damage, which was extended into major rips by canopy buffeting, occurred at Mach 3.3 (ref. 59).

2.2.4 Reefing-Design Parameters

Reefing of parachutes and parachute-like decelerators to limit peak loads and decelerations is accomplished almost exclusively through restriction of the air inflow at the canopy mouth by means of a temporary line around the skirt. This method, known as skirt reefing, has proven to be highly reliable even though four or more stages of reefing may be needed to obtain effective control of area growth. The primary reefing-design parameters are the reefing ratio (D_R/D_O , or diameter of reefing line circle/canopy nominal diameter) as given in figure 7 and the operational interval(s) over which the parachute remains reefed. The typical variation of effective drag-area ratio with reefing ratio is given in figure 7.

2.2.5 Weight and Packaging

The parachute is the lightest and most efficient means known for providing a large drag surface for a spacecraft. Moreover, the steerable parachute affords the most efficient lifting surface for low-glide ratios (L/D max = 0.8 to 1.1). The weight of deployable decelerators generally increases in proportion to their complexity (requiring additional components) and the severity of their opening shock (requiring stronger and therefore initially heavier materials). Available literature on decelerator-engineering data includes curves that give weight as a function of size for specific structural classes. Where more accurate results are needed, the weight of a given decelerator design is calculated from the dimensions of each component and the unit weights of materials.

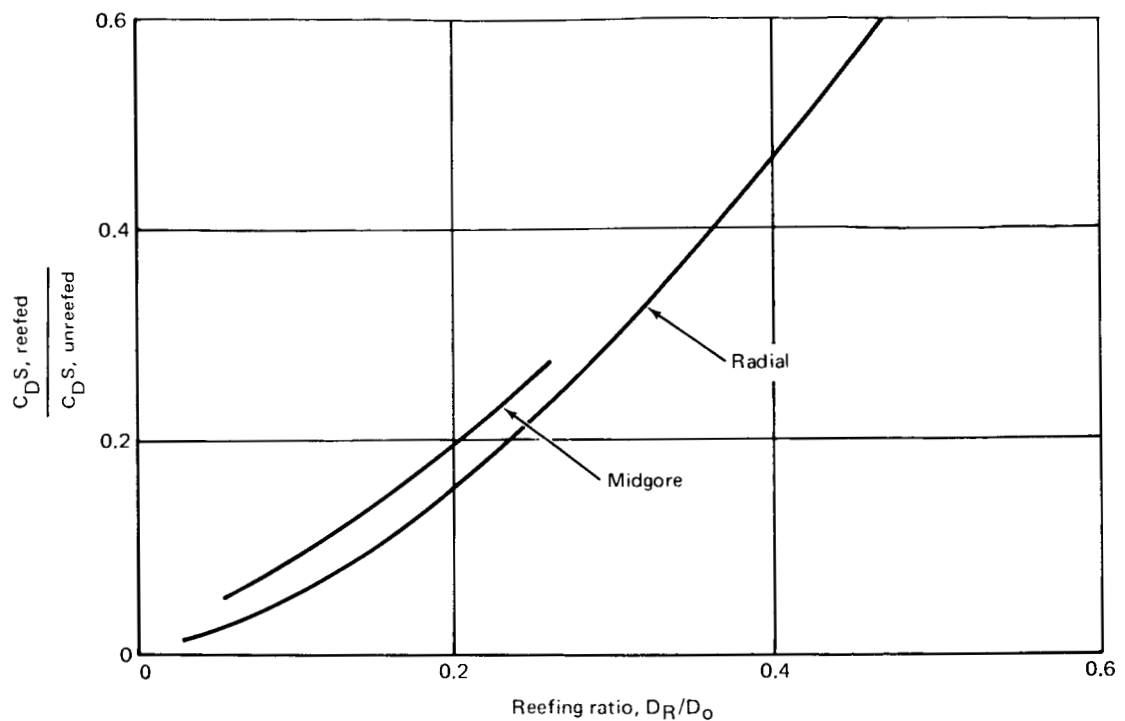


Figure 7. — Variation of effective drag-area ratio with skirt-reefing ratio for a typical decelerator.

The packed volume of the decelerator assembly is calculated from the weight and average packing density. The density of the package depends on the packing method used, as well as on the pliability, resilience, and specific gravity of the basic materials. For nylon parachutes and similar structures, the established practical density limits are given in table II.

TABLE II. — PACKING DENSITIES OF NYLON DECELERATORS

Packing method	Pack density	
	kg/m ³	lb/ft ³
Manual		
soft	352	22
hard	448	28
Vacuum or light		
mechanical press	481	30
Pneumatic press	561	35
Hydropress		
light	641	40
medium	738	46

The density of solid nylon is 1138 kg/m^3 (71 lb/ft^3); Dacron and Nomex, both with a 21-percent greater density than nylon, have proportionally higher packing densities. A decelerator is generally first packed in a strong box having the same shape as the spacecraft compartment in which it will later be stowed. The inside dimensions of the box are such as to provide for a fraction-of-an-inch clearance all around between the pack and the compartment. (One exception is the frequent use of a deployment mortar, both as a packing box and as a parachute shipping container.) A deployment bag of the same size and shape as the box is inserted into the packing box. The decelerator is progressively S-folded and compressed into the bag in an order opposite to its order of deployment (e.g., the canopy apex first, then suspension lines and risers). Parachute packs of many shapes have been used successfully; however, odd-shaped packages have proven more difficult to pack to a uniformly high density.

The tendency of flat-sided packs to bulge and expand after removal from the packing box (making insertion into the stowage compartment of the space vehicle difficult) has been overcome in several different ways: (1) by storing the pack in a tight-fitting shipping box designed to preserve its dimensions; (2) by sealing the pack in an evacuated bag of polyethylene film; or (3) by packing under both pressure and heat. The third method, an autoclave process, sets the dimensions of the pack so that no subsequent expansion takes place (ref. 60).

2.2.6 Ejection, Deployment, and Inflation Control Devices

Two basic types of parachute *ejection devices* have been employed in spacecraft systems: (1) those which forcibly eject the pack at a substantial velocity and (2) those which extract the pack from its compartment by drag and/or momentum.

Ejectors include mortars and ejector bags. Mortars are efficient devices that can eject decelerator packs at muzzle velocities of 30.5 to 61 m/sec (100 to 200 fps). The weight of deployment mortars used in spacecraft systems is approximately one half to one third that of the pack, as illustrated in figure 8 for mortars having aspect ratios of 1 to 2.5. The weight of a pack that can be ejected by a mortar is limited only by spacecraft design constraints on reaction loads and package shapes.

The ejector bag is an impulsively inflated envelope, capable of ejecting a heavy pack from its compartment at a moderate velocity to aid pilot-chute deployment of the main-descent surface. The ejector bag is an effective means of preventing the type of contacts with vehicle structure that delay pack extraction when the spacecraft is in an unfavorable attitude. This consideration becomes increasingly important as the size and weight of the main pack are increased, and is crucial in abort modes where the deployment time must be as short as possible.

The extraction type of *deployment devices* includes the slug gun, which uses the momentum of an ejected slug to extract the pilot chute and small drogues, and the

pilot chute itself, which uses drag as an extraction force. Drogue chutes have also functioned reliably to extract main-parachute packs at the conclusion of the drogue's working interval. Specialized thrusters, catapults, and pilot-drag devices of other types have been utilized in decelerator systems, but their weight efficiencies tend to be relatively low.

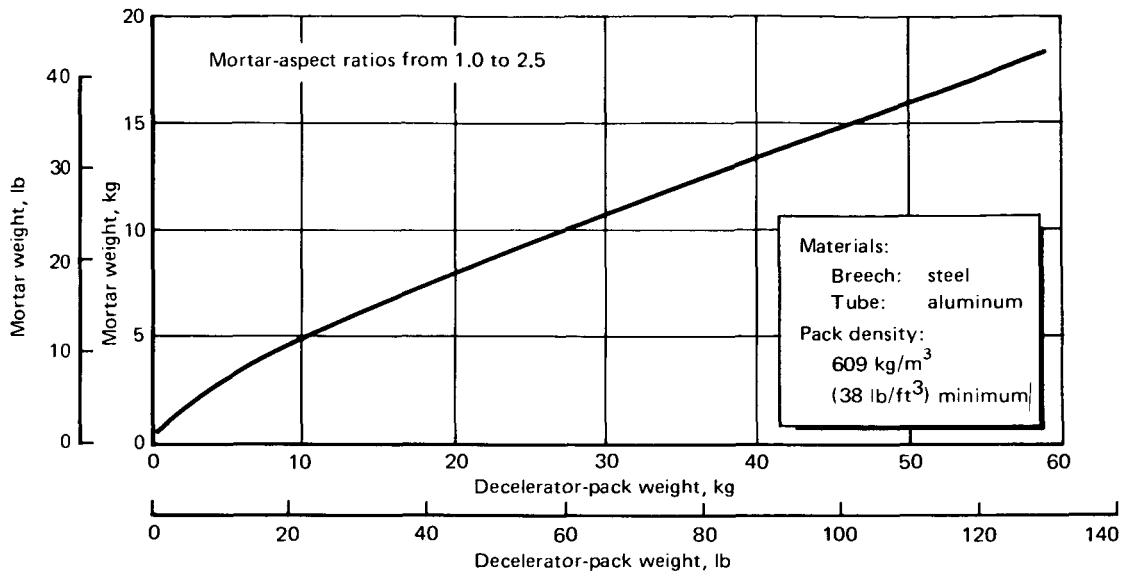


Figure 8. — Mortar weight versus weight of decelerator pack.

The deployment bag is widely used to package the deployable decelerator. Its primary purpose is to control payout of risers and lines, and to prevent the mouth of the canopy from opening prematurely during stretchout, thereby minimizing the "snatch force." Two basic types of deployment bags are in general use: (1) strong, compartmented bags for deployment by extraction and (2) lighter, noncompartmented bags for deployment by an ejection device (mortar).

The compartmented bag contains internal flaps to retain the canopy. The flaps are locked in a closed position by fabric loops in which the first group of line bights is stowed. The suspension-line compartment contains rows of stowloops or other means of securing short bights of the lines snugly in position for orderly extraction. Textile risers are stowed in the line compartment under the bag-closure flaps; generally, risers of flexible steel cable are stowed outside the bag. The bag-closure flaps are locked by a variety of means (webbing loops or breakaway lashings), but all closure-flap locks are designed to be opened, cut, or simply broken by a special fitting (webbing loop or knife ring) when the external riser becomes taut during deployment. Because high-velocity extraction of the decelerator may cause frictional-heating and abrasive damage, most deployment bags are lined with a smooth material (such as teflon fabric) to minimize friction. A noncompartmented bag may contain a lead disk or mortar sabot attached to the bottom to augment strip-off momentum (ref. 2).

The most commonly used *inflation-control devices* are pyrotechnic reefing-line cutters. These cutters are available with delay times ranging from one to sixteen seconds and longer, and in various sizes with capabilities of severing reefing lines ranging in tensile strength from 44 500 to 890 000 N (1000 to 20 000 lbf).

Similar pyrotechnic guillotines, as well as a variety of mechanical release devices, are used at decelerator termination. These devices have been developed and tested for severing the lines of both heavily loaded drogues and lightly loaded main parachutes or lifting surfaces. In steerable systems, the lines severed after touchdown include control as well as main riser or harness members.

Specialized step-release deployment hardware has been developed for deployable wings, for which the lengths of all suspension lines must be equalized to improve the distribution of deployment and opening loads (refs. 13 and 41). To prevent fouling, the slack portions of equalized lines are usually stowed in a series of tubular channels adjacent to the step-release units. These units are actuated after the final reefed stage to bring the deployable wing into flying trim.

2.2.7 Sensors and Controls

Deceleration-system deployment and other functions such as drogue disconnect and termination of system operation are initiated by a variety of sensors and electronic and mechanical controls, including altitude-sensing baroswitches, radar absolute-terrain-clearance transducers, accelerometers, base-pressure and ram-pressure transducers, and inertia switches. Sequencing of a series of decelerator events is controlled both by electronic timing devices and by simple mechanical links such as lanyards and bridles. Wherever reliability considerations warrant, sensors of different types are placed in parallel to ensure initiation and in series to prevent premature initiation. On manned spacecraft, automatic decelerator controls are made subject to manual override.

In steerable-parachute and deployable-wing systems, glide modulation and turning is generally controlled by electric winches which extend and retract control lines. Both proportional and step (so-called "bang-bang") control systems have been used in flight tests (refs. 41, 45, and 46).

2.2.8 Materials

The materials used in deployable aerodynamic deceleration systems are generally woven textiles of high strength-to-weight ratio and cloths of various porosities ranging from zero to roughly 50 percent. The fibers used in spinning yarns for these textiles include nylon, Dacron (ref. 61), Nomex (ref. 62), cotton, glass, stainless steel, or René 41 (ref. 63). The textiles may be coated with various pliable substances which provide for low friction, abrasion resistance, zero permeability, or increased heat resistance, as required. Representative coating materials include neoprene, silicone rubber, Armalon 98-101 (ref. 64), and special formulations of polyurethane (refs. 10 and 27).

The mechanical properties of nylon provide the toughness, strength, high energy-absorbing capacity, and low weight required of decelerator textiles. High-tenacity Dacron has similar properties but is somewhat heavier (about 1/5 heavier) and has a smaller energy-absorbing capacity (about 70 percent) above 373K (100°C) (refs. 65 to 67). Nomex (a type of nylon) is used where strength retention at elevated temperatures is required (fig. 9) because it retains over 50 percent of its room-temperature strength at 523K (482°F), the temperature at which both nylon and Dacron melt. Nomex has about 65 percent of the strength of nylon and high-tenacity Dacron at room temperature, and is 21-percent heavier than nylon.

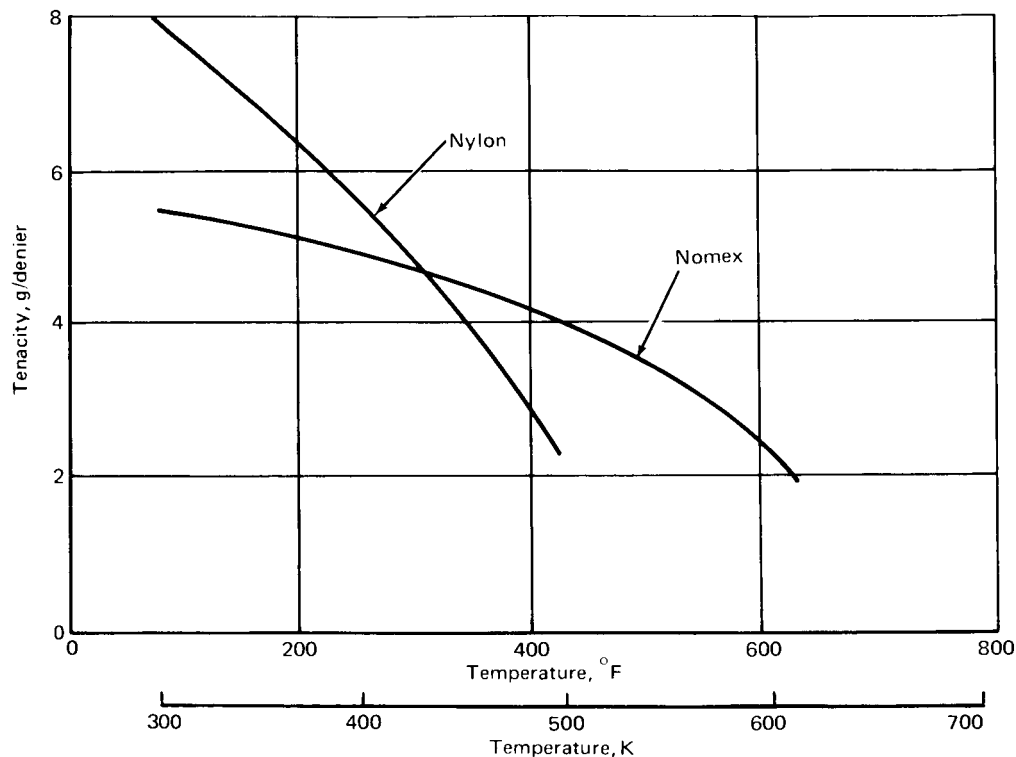


Figure 9. — Strength of nylon and Nomex at elevated temperatures.

The static stress-strain characteristics of nylon, Dacron, and Nomex are highly nonlinear (e.g., fig. 10). Hysteresis is large for these synthetics, and complete recovery after the removal of the applied load requires several hours (ref. 65). Moreover, the stress-strain and hysteretic characteristics vary with the rate of load application (ref. 68). Extensive work remains to be done before the response of nylon and similar materials to dynamic loading conditions is adequately understood. Present methods of stress analysis, for example, still depend on material strength and load versus elongation data derived from static tests.

The air permeability of decelerator fabrics varies widely because of manufacturing tolerances, and during operation increases with increasing differential pressure (fig. 3).

The rated air permeability of cloth is expressed in cubic meter per minute per square meter (cubic foot per minute per square foot), measured at a differential pressure of 1.27 cm (0.5 in.) of water. Described in velocity units, the permeability rating represents the average velocity of airflow through the fabric.

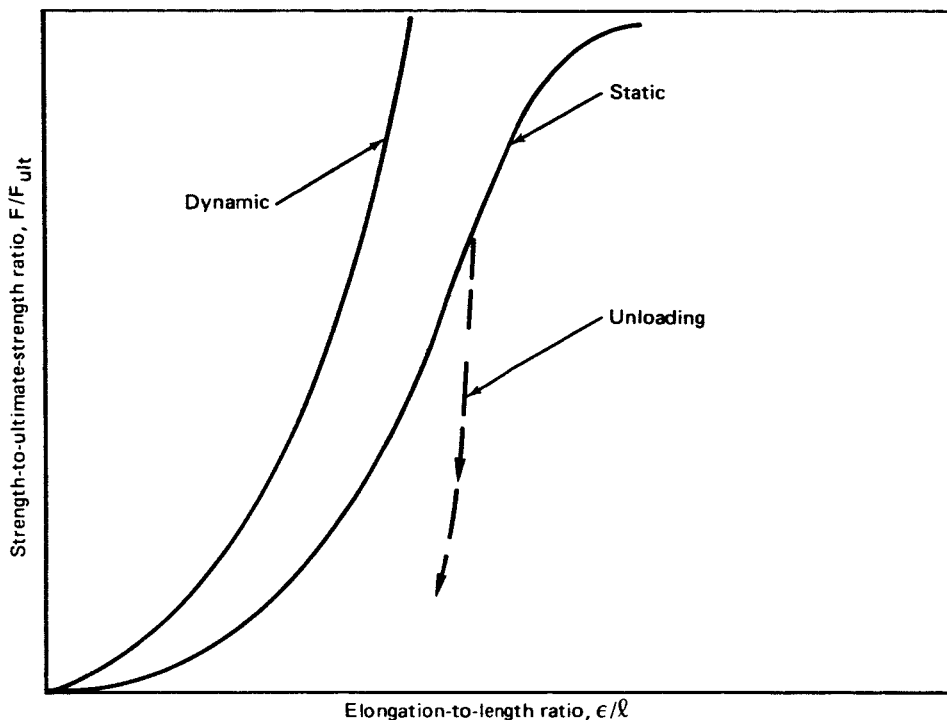


Figure 10. — Load-elongation characteristics of nylon textiles.

A more useful concept is that of relative porosity, expressed as the ratio of the average through-flow velocity to freestream velocity, usually in percentage. In this form, permeability or fabric porosity is directly comparable to geometric porosity, which is the ratio of the open area (slots and vents) to total area of the canopy surface, also expressed as a percentage. Because of the effect of increasing pressure, correlation of decelerator aerodynamic characteristics with cloth porosity can be expected only at low steady-state velocities, and not during opening and deceleration, where differential pressures are considerably higher than the standard value of 1.27 cm (0.5 in.) of water.

2.2.9 Fabrication Processes

Fabrication processes employed in deployable aerodynamic decelerator technology include measuring, laying out, cutting, machine stitching, and manual lashing and rigging. All cords, tapes, ribbons, and webs are measured under tension before cutting, but cloth is not. Cloth is rolled off the bolt, smoothed, and stacked in multiple layers on a table. A pattern is superimposed, and all layers are cut at once with a power shear.

Because the machine-stitching process causes some gathering along seams, the pattern may include a shrinkage allowance when specific finished dimensions are required.

Standard seams are made with one to four rows of stitching; each seam is sewn in a single pass through a multiple-needle machine. The quality of the seam with respect to straightness, uniformity of fold, and gather depends largely on the skill of the sewing-machine operator. Seam-forming aids are used and automatic sewing machines are available for a variety of frequently used stitch patterns. Sewing machines are made to operate in different capacities ranging from light to heavy, each having characteristic upper limits in the sizes of threads and thicknesses of seams it can accommodate. As late as 1967, the technology of assembling stainless-steel textiles had not been adequately developed (ref. 15), and its present status is uncertain.

Manual assembly operations include attaching suspension lines to radial loops, forming attachment loops, threading cord through fabric channels and reefing rings, hand stitching reefing-line joints during packing, tying cord to metal fittings, assembling separable links, and performing a variety of packing and rigging tasks.

Quality of manufacturing is controlled by several means, including the following:

- Certification or laboratory testing of raw materials
- Inspection of received materials to detect defects (100-percent inspection is preferred for applications not requiring the production of a very large number of decelerators where sampling techniques may be used.)
- Frequent inprocess inspections using light tables and other visual aids
- Detailed examination and measurement of final assemblies
- X-ray inspection of high-density pressure packs
- Proper training of all working and operational personnel
- Step-by-step control of rigging and packing procedures in accordance with detailed checklists
- Proper maintenance of equipment and sewing machines to ensure good working condition
- Use of air-conditioned workrooms
- Good housekeeping with a high standard of cleanliness

2.2.10 Advanced Decelerator-Design Problems

The development of advanced deployable aerodynamic deceleration systems has been beset with special problems which limit the designer's ability to predict the performance of such systems. One such problem is that the behavior of a deployable aerodynamic decelerator changes significantly with scale in a manner that limits the absolute size of a successful configuration. As noted in Section 2.2.1.6, the complexity of the decelerator structure prevents characterization of its aerodynamic scale in simple terms. Several Reynolds numbers may be identified; for example, those for flow around the mouth of the inflating canopy, through the pores of the fabric, through the slots and vents, and around the fully inflated canopy. The result is that size-limiting scale effects cannot be predicted on the basis of Reynolds number alone, and empirical methods have been relied upon to establish the limits of absolute size and to validate methods of raising such limits for specific decelerator types. Following are examples of these methods.

- A reduction in opening tendency with increasing scale to a size beyond which full inflation cannot be obtained occurs in ventilated-canopy designs and those having inverted conical or in-curved shaped skirts. In ribbon and ringslot canopies, such "squidding" is prevented by reducing the total porosity of the canopy as the size is increased; ribbon parachutes in sizes up to 39.7-m (130-ft) diameter have been successful. In extended-skirt canopies, squidding has been prevented through the use of pocket bands (ref. 7) and an increased angle of attack of the skirt; extended-skirt parachutes with pocket bands in sizes up to 30.5-m (100-ft) diameter have been successful, while smaller models without pocket bands have failed to open. Since the hemisflo-ribbon canopy has an in-curving extended skirt in a ventilated surface and is currently being made without pocket bands, the probability of making successful models much larger than $D_0 = 4.9 \text{ m}$ (16 ft) appears small.
- Large-scale decelerators are usually constructed of the same materials as small models. One of the consequences is an increase in the relative elasticity of the structure (refs. 69 and 70). This is generally beneficial to the performance of conventional parachutes but not to the performance of steerable gliding systems where both inflexibility of coupling between surface and vehicle and dimensional stability are of utmost importance. Coupling flexibility degrades the controllability of the gliding system in maneuvers, while different elongations under successive opening loads produce hysteretic effects on the lengths of suspension lines that may modify the flying trim of the surface (ref. 65). While both the effects of elasticity and of hysteresis may lead ultimately to configuration changes in large-scale gliding systems relative to presently successful smaller systems, it is known that the effects of hysteresis alone have not as yet caused flight problems of any consequence in parawings of a 372-m^2 (4000-ft^2) surface area (ref. 13).

Various advanced decelerator designs are based on the clustering of two or more canopies. Clusters have a shorter total filling time than a single large parachute and present the possibility of realizing a high reliability without 100-percent redundancy; for example, a high degree of reliability is ensured in the Apollo main parachute system by a 50-percent redundancy since any two of the three canopies can satisfy the landing requirements (refs. 1 and 31). However, clustering can cause undesirable effects, including a loss of drag efficiency in steady descent and unequal load sharing among the members of the cluster during opening. Consequently, the design load for each parachute in the cluster is relatively high, and the system weight is greater than that of an equivalent single parachute (ref. 71).

The tandem-canopy configuration is used in some deployable deceleration systems. The trailing canopy may be a pilot chute used to stabilize deployment of the main canopy and to mitigate reefed opening loads, or it may be a target canopy for aerial recovery. The performance of this kind of system varies with the relative sizes of the two components and the distance between them. The operation of the pilot chute attached to the apex of the main canopy is transient, ending with collapse of the pilot chute in the wake of the main canopy. However, when the attached pilot chute is large, relative to the main canopy, its drag is sufficient to modify the opening process of the main canopy to a marked degree, causing squidding in extreme cases. On the other hand, the trailing target canopy must maintain a stable inflated shape at a fixed point over the main canopy. This is accomplished by various arrangements, including a directionally stabilized target canopy with a control tow line of considerable length or a multiple-line system that holds the target canopy closely over a large central vent in the main canopy.

The problem in designing an advanced tandem-canopy configuration of either type is that very little quantitative data exist to support prediction of the effects of relative size and relative trailing distance of the two canopies on the filling times, opening forces, drag, and stability of either member canopy or of the tandem system as a whole. This deficiency in data does not, however, appreciably affect the design of gliding parachutes, deployable wings, and other systems in which the pilot chute is not retained after deployment.

A special problem in deployable decelerator design is presented by the inordinate complexity of the behavior of flexible aerodynamic structures during inflation and under dynamic-loading conditions. As a consequence, they cannot be analyzed with the same rigor with which aircraft or spacecraft structures are treated; there is virtually no dependable intermediate approach between the approximate empirical methods used and the presently insoluble rigorous mathematical formulations dictated by theory. Although the empirical methods are inaccurate and cannot be applied to conditions outside the area of test experience, they are amenable to improvement (e.g., refs. 55, 57, 70, 72, and 73) and remain more useful and dependable than the numerous oversimplified but still complex analytical methods (e.g., refs. 7, 27, 74, and 75).

2.3 Selection Procedures

Selection of candidate deceleration systems for a specific spacecraft mission is made on the basis of (1) a comparative analysis of the existing knowledge concerning each candidate relative to the anticipated operating conditions and (2) comparative testing of models to generate quantitative data that will support the choice from among the most promising candidates. The first approach is applied to a wide field of possible systems; the second is applied to the two or three most promising candidates when existing knowledge is not sufficient to support a decision through analysis alone.

A value matrix is generally used to establish figures of merit for the candidate systems based on all pertinent operational factors, including (1) decelerator-weight efficiency, (2) maximum packing density, (3) deployment characteristics, (4) special limitations or requirements, (5) inflation reliability, (6) stability, (7) snatch- and opening-load factors, (8) static and dynamic stability, (9) load oscillations, (10) staging and reefing requirements, (11) repeatability of performance, (12) control response, (13) backup requirements, (14) complexity, (15) decelerator-system reliability, and (16) development status. Inputs to the selection process may also be derived from parametric analyses which provide system-optimization data, indicate possible differences in growth potential, or establish the sensitivities of competitive designs to economic factors. Quantitative evaluations are used wherever possible, but dependence on the qualitative judgment of experienced engineers is unavoidable in many cases. Care must be exercised, however, in the application of new concepts. In the case of the Gemini program, for example, the use of an advanced decelerator system (paraglider) had to be abandoned during the development phase and an alternate parachute decelerator used in lieu of the paraglider as the primary landing system. It is generally recognized that the plan to use the paraglider was premature.

Comparative model testing of candidate decelerators is performed almost exclusively in the wind tunnel, but this is not always adequate for simulation of critical dynamic conditions. Consequently, comparative aerial-drop testing is also conducted occasionally. The great majority of wind-tunnel tests are performed under "infinite-mass" conditions because simulation of the deceleration that occurs during finite-mass operation is difficult.

2.4 Calculation of Design Loads and Stresses

Generally, approximate empirical methods (described in ref. 7) are used to calculate decelerator loads and stresses. On the other hand, a good deal of theory has been developed to support an analytical approach to parachute-deployment and -opening loads (refs. 70 and 76 to 78), but the large number of variables associated with the inflation, loading, and operation of flexible fabric structures lead to analytical formulations that thus far have defied solution by any means. Consequently, the usefulness of mathematical models depends heavily on empirical data derived mainly from full-scale aerial-drop tests. References 70 and 72 describe some improved

mathematical methods validated by Apollo parachute-test data. Data generated by three to six aerial-drop tests of the right kinds can support the prediction of design loads and stresses with an accuracy of roughly ± 10 percent by the approximate methods and ± 5 percent by the improved methods.

2.4.1 Prediction of Opening Loads

Probable maximum opening loads are estimated by various computational procedures derived from the so-called "opening-shock-factor" method, (renamed the "opening-load-factor" method). The method provides a simplified analytical approach that yields quick and dependable results when carefully applied and when pertinent empirical data are available. There are some documented test data for most of the decelerator types listed in table I, and appropriate references are given. Data on measured opening loads, drag areas, system weight, and flight-test conditions are required. The quantity of such data must be sufficient for plotting curves of the types illustrated in figure 2f (or similar curves relating the opening-load factor to unit-canopy loading). The data must span the operational conditions of the decelerator being designed. Application of the load-factor method of predicting opening loads is illustrated in reference 34 for single parachutes, in reference 32 for aerial-recovery parachutes, in references 70 and 71 for cluster parachutes, and in reference 13 for the parawing. Some typical opening-load factors for the "infinite-mass" loading case are given in reference 7 for different types of parachutes.

Other more complex analytical methods for predicting opening loads are cumbersome, time consuming, and undependable outside the particular framework (decelerator model and types of test data) for which they were derived (ref. 1). The method of predicting ballute-opening loads is described in reference 27.

New analytical tools in the form of specialized digital-computer programs for the prediction of parachute-opening loads are being developed and should become increasingly available throughout the next few years (e.g., ref. 70). Cyclic acceleration of the towed decelerator caused by vehicle oscillation can be a contributing factor to peak opening loads. A computer method for evaluating spacecraft oscillations during decelerated descent and the effect of these oscillations on decelerator loads are reported in reference 79. This method uses a digital-computer program written in three degrees of freedom around a complex model which includes descriptors for atmospheric properties, decelerator inflation and disreef processes, and harness-attachment geometry. The nature of the increase of parachute-opening shock with altitude is indicated in reference 80, but a dependable method of predicting the effect without supporting test data does not exist.

2.4.2 Stress Analysis

One advanced method of parachute-stress analysis developed for annulate canopies (i.e., the polysymmetric ribbon, ringslot, and ringsail parachutes) is given in reference

72. The mathematical model used in this method includes the dimensions of every structural member in the parachute, together with the stress-strain characteristics of each different material, the pressure distribution across the canopy (derived from empirical data similar to that given in ref. 81), the applied-riser load, and the shape of the canopy at the time of the peak-riser load. Digital-computer evaluations of strain versus stress are iterated until the shape of the canopy computed from a stress-strain evaluation agrees with the observed shape and the computed net pressure load agrees with the applied load. This computation provides a tabulation of internal loads for each structural member with sufficient accuracy to identify critical areas and probable points of failure. This enables optimization of the structure for consistent margins of safety throughout the canopy. A similar method applicable to parawing and other surfaces that are not polysymmetric is in an advanced stage of development (ref. 14).

Less rigorous empirical methods for stress analysis of parachute structures are described in reference 7, and their uses are illustrated in references 4, 15, 34, and 75. With these methods, estimates can be made quickly of the required strength of materials for major members of the parachute structure, such as harness, risers, suspension lines, canopy radials, canopy fabrics, circumferential bands, and reefing lines.

The stress analysis of deployable wings by methods other than that described in reference 14 requires a cautious basic approach guided by applicable membrane theory (e.g., ref. 82), with heavy reliance on laboratory and aerial-drop tests. Structural design of ballutes and attached inflatable decelerators is based on the theory of isotenoid surfaces described in references 8 and 27. The isotenoid analysis yields accurate results for only one set of deployment conditions. Moreover, internal loads calculated through isotenoid analysis are not the critical loads for structural design. Critical loading of ballutes is not amenable to analytical treatment because the highest stresses result from fluttering and whipping ("flagging") during inflation. Because of this major uncertainty, large design factors derived from test-damage experience are applied to the calculated loads. A major problem in the calculation of stresses is the lack of knowledge of the magnitude of transient aerodynamic pressures and forces.

2.5 Tests

Test evaluation of systems, components, subassemblies, and materials constitutes a large and important part of the design-development and qualification task for most deployable aerodynamic decelerators. On the basis of experience with Discoverer, Mercury, Gemini, Apollo, ASSET, Biosatellite, etc., the numbers of various types of tests to be planned for a typical decelerator program are approximately as follows: wind tunnel, 50 to 100; development (laboratory), 250 to 500; development (full scale, aerial drop), 40 to 80; verification of flight loads (full scale), 10 to 15; and qualification (full scale), 8 to 12. Acceptance tests have dealt mainly with verification of the mechanical properties of numerous raw materials. Salient features of the state of

the art in decelerator testing as they apply to systems and components, materials, joints, seams, attachments, and reinforcements are summarized in Sections 2.5.1, 2.5.2, and 2.5.3.

2.5.1 Systems and Components

Individual decelerator assemblies and complete systems are customarily subjected to tests designed to verify function, performance, and structural integrity in each functional mode from deployment to termination of operation.

Objectives of laboratory tests performed on systems and components include:

- Development of packing and rigging procedures
- Simulated extraction and deployment on the packing table
- Static mortar firing and similar powered tests of deployment devices
- Simulation of operational sequences
- Evaluation of environmental and aging effects on complete decelerator packs

Small-scale decelerator models and, where feasible, full-scale prototypes are tested in the wind tunnel under both steady-state and dynamic conditions, with heating included, as applicable, to determine the effects of various design parameters on such performance characteristics as filling times, opening shock, drag coefficient, and static and dynamic stability derivatives. Usually, only comparative evaluations can be made with wind-tunnel test data because of uncertainty as to the applicability of the various scaling laws to quantitative interpretation of the results.

System and component tests may also be performed by towing small-scale decelerator models and, where feasible, full-scale prototypes, with vehicles of various types, including automotive trucks, rocket sleds, and aircraft. For the test, the vehicle is equipped with suitable superstructures or tethering apparatus as well as instrumentation for measuring such decelerator characteristics as applied loads, attitude, canopy-shape stability, and response to control functions.

Flight testing of both small- and large-scale decelerator models is the most widely used method of demonstrating that a component or a decelerator system will operate as designed under the wide variety of conditions that can be encountered. The flight-test vehicle can be any one of the following:

- A weight bomb or dummy vehicle launched from aircraft (refs. 1, 7, and 54)
- An instrumented projectile launched by rocket (ref. 26)

- An instrumented dummy vehicle carried aloft by a balloon before acceleration to high altitude and velocities by a rocket (ref. 83)
- An unmanned entry vehicle or capsule launched into simulated entry trajectories

Flight tests should duplicate as much as practicable the interface between spacecraft and recovery systems. Wake drag, payload dynamics, and payload geometry, for example, can have important effects on the performance of the system.

Flight-test instrumentation includes an assortment of onboard, airborne, and ground-based motion-picture cameras of various frame rates; decelerator-force transducers; vehicle-acceleration transducers; pressure and temperature transducers, as required; photo-theodolite tracking and ranging equipment; and special-purpose instruments (ref. 7).

Before conducting flight tests of a new decelerator design with instrumented vehicles, it is customary to perform a simple functional drop test with a low-cost weight bomb to ensure that the new decelerator will inflate and operate essentially as intended. Also, before performing complex dynamic tests at extreme conditions, several dynamic tests are usually performed under moderate conditions to establish the normal performance characteristics of the decelerator — unless an adequate frame of reference has already been established by prior test experience.

It is not economically feasible to perform the full number of tests required for an unqualified definition of the static and dynamic characteristics of a given deployable aerodynamic deceleration system. The compromise usually made is to test at the critical boundary conditions of the performance envelope as thoroughly as program funding will allow. Sometimes, however, a more comprehensive test program is unavoidable. At such times, scaling laws (e.g., ref. 69) and statistical analysis are used to determine the configurations and conditions which should be evaluated to produce a maximum yield of useful information from a limited number of tests.

2.5.2 Materials

The mechanical and physical properties of materials and the effects of various environments on these properties are evaluated in laboratory tests. Testing apparatus includes the following:

- Machines for testing tensile strength, tearing strength, fatigue, and abrasion
- Devices for measuring the air permeability of the fabric at various differential pressures, both unloaded and under biaxial loading (ref. 65)
- Vacuum and heating environmental chambers

- Specialized impact- and dynamic-loading equipment (refs. 66 to 68)
- Chemical or hot-gas sterilization chambers

2.5.3 Joints, Seams, and Reinforcements

The laboratory equipment used for material testing is also used to evaluate the efficiencies of joints and the load-transfer characteristics of the various types of attachments, seams, and reinforcements employed in textile structures. While they are not commercially available, special-purpose jigs, fixtures, and dynamic-loading apparatus, which provide a good simulation of both static and dynamic loads applied to large specimens, have been assembled both by contractors and Government agencies. Equipment has also been assembled to meet the specific need for testing specimens under variable strain rates.

3. CRITERIA

The deployable aerodynamic deceleration system shall be designed to decelerate, stabilize, and control the descent of the spacecraft in the service environment within prescribed limits without imposing detrimental loads, deformations, vibrations, or impact shocks on the deceleration system or the spacecraft.

Loads and stresses imposed by deployment shall be determined by analysis and test. Loads and stresses induced in the deployable decelerator shall be determined by analysis and test. Structural design factors shall be defined and applied to the deployable deceleration system to account for known deleterious phenomena. Safety factors shall be applied to limit loads to determine the ultimate loads which the decelerator system shall withstand without failure.

3.1 Functional Considerations

The deployable aerodynamic deceleration system shall be designed to perform the following functions:

- Deploy and inflate under specified operational conditions through an orderly sequence of stages.
- Decelerate the spacecraft in accordance with a specified velocity decrement through an orderly sequence of stages.
- Stabilize the spacecraft within acceptable angular position and rate limits through each operational phase.

- Control the vertical and horizontal velocity of the spacecraft during steady descent in still air within specified limits
- Be responsive to control signals appropriate to the decelerator's designed functions

If required, the system shall also be capable of:

- Sustaining engagement of the recovery pickup system and acceleration to recovery aircraft speed, maintaining a stable towing configuration afterwards, and limiting parachute damage during reel-in and boarding to an acceptable level. The parachute shall be capable of reinflation and satisfactory descent to the surface in case of disengagement.
- Performing a terminal-deceleration or landing-flare maneuver to touchdown in a safe and stable manner.
- Terminating decelerator operation by disconnecting in a manner that will have no unfavorable effects on the subsequent motion or condition of the spacecraft.

The probability that all these functions will be performed without functional or structural failure shall be consistent with the overall reliability required of the spacecraft and its mission. All functions shall be performed in a manner compatible with the functions of other spacecraft systems.

3.2 Design Characteristics

Design of the deployable deceleration system shall, as a minimum, account for the following system characteristics:

- Aerodynamic characteristics of the spacecraft during deployment and operation, including lift, drag, stability, damping, wake flow, and ballistic coefficient
- Aerodynamic characteristics of the decelerator system, including
 - (a) Basic characteristics such as size, type, lift, drag, stability, and damping
 - (b) Size-limiting scale effects
 - (c) Cluster effects
 - (d) Attached pilot-chute effects
 - (e) High rate of onset shocks

- Material, physical, and mechanical properties and their variability (Values for properties of decelerator materials shall be obtained from sources approved by NASA. Materials shall be characterized in sufficient detail to permit high-confidence predictions of material properties.)
- Dimensional stability of textile structure
- Effects of high-density packing
- Effects of ejection or extraction system
- Effects of decelerator deployment
- Location, shape, and volume of allocated storage space(s)
- Number, type, and location of decelerator-system-to-vehicle connections

3.3 Operational Conditions

Design of the deployable deceleration system shall, as a minimum, account for the following operational conditions:

- Static and dynamic loads and pressures induced in the decelerator system by deployment and operation
- Mass and inertial properties of the spacecraft and decelerator system
- Temperatures induced by deployment, operation, and storage
- Composition and properties of the atmosphere, especially the density-altitude profile
- Winds and gusts
- Natural and induced environment
- Planetary gravity effects, if applicable
- Effects of sterilization, if applicable

3.4 Design Constraints

The design shall account for constraints imposed upon the overall system which may include requirements or limitations on any of the following:

- Structural or functional limitations imposed by the spacecraft
- Spacecraft deceleration, shock, vibration, and orientation
- Size and weight of the decelerator system
- Sink speed at a given altitude
- Aerial recovery
- Vertical velocity at touchdown
- Horizontal range
- Controllability
- Stability
- Produceability
- Communication, location, and retrieval during and after the descent phase
- Refurbishment, repair, and maintainability and reuse
- Safety
- Reliability

3.5 Selection

A rational selection of the type of deployable decelerator to be used shall be based on a systematic evaluation that accounts for functional requirements, design characteristics, operational conditions, and design constraints.

3.6 Design Analysis

Analytical models of the deployable aerodynamic decelerator shall be used to determine, as a minimum, the applied loads, size, strength, weight, and volume of the decelerator components and the operating characteristics of these components. Analytical models shall include representations of the following particulars, as applicable:

- Flight trajectory of the spacecraft during sequential operation of the deceleration system

- Decelerator-opening loads
- Effects of spacecraft attitude-change rates on decelerator function and loads
- Deployment (snatch) forces and reaction loads
- Internal loads and stresses
- Structural design factors
 - (a) Derating factors shall be defined and applied to allowable strength levels of decelerator materials to account for such known deleterious phenomena as abrasion, fatigue, environment (temperature, humidity, vacuum, radiation, etc.), joint efficiency, nonuniform loads, and line convergence.
 - (b) Safety factors shall be defined and applied to limit loads to determine ultimate loads. A safety factor shall be used only to account for design uncertainties that cannot be rationally analyzed or accounted for by other means; for example, residual stresses, uncontrollable degradations due to manufacturing processes, and uncertainties in the rate of application of load.
- Number, timing, and sequence of decelerators and deceleration stages between deployment and touchdown
- System-stability characteristics during decelerated flight, near-equilibrium descent, and controlled flight
- Spacecraft-wake effects
- Dynamic-heating effects
- Aerodynamic performance of deployable wings
 - (a) Turning rate and L/D-modulation range and rate
 - (b) Sinking speed as a function of turning rate and L/D modulation
 - (c) Relative motion of spacecraft and main sustaining surface during maneuvers
- Component and system reliability

3.7 Tests

Test data shall be used to validate the physical and mechanical properties of materials, system and component designs, and analytical models used in the design calculations.

As a minimum, the following material characteristics and mechanical properties shall be verified by test or test data:

- Ultimate strength and elongation
- Stress versus strain
- Tear resistance
- Crease resistance or resilience
- Fabric porosity at operating conditions
- Unit weight

The calculated effects of natural and operational environments on all critical characteristics of materials shall be validated by tests or test data. Standardized and consistent testing methods compatible with the application of the material shall be used.

The function, performance, and structural integrity of decelerator systems and components shall be validated by tests or test data.

The calculated effects of the operational environments and other design conditions on all critical design characteristics shall be validated to the fullest possible extent by tests or test data.

4. RECOMMENDED PRACTICES

Selection and design of a deployable aerodynamic deceleration system demands careful integration of a complex of interfaces between the system and the spacecraft, and satisfaction of a large number of requirements and constraints, some of them conflicting. Consequently, continuing coordination and consultation are essential among the various design groups working on the same spacecraft, particularly those concerned with structures, landing gear, electrical subsystems, controls, and location and retrieval aids.

A good first step in the selection and design of a deployable aerodynamic deceleration system is to make sure that all information pertinent to formulation of the basic-design

inputs for a specific system is available to the designers. It is a common mistake to underestimate the types, quantity, and detail of such information needed at the outset to perform an adequate analysis of the deceleration-system design. Preliminary design analyses of candidate systems, supported by an understanding of decelerator functions, should be performed as a basis for analysis of system, component, and detailed configuration requirements for the selected system. System, component, and detailed-configuration analysis, in turn, produces a firm basis for evaluating the effects of operational conditions on decelerator design.

4.1 Functional Considerations

In preparation for the detailed recommendations, a summary is presented here of the methods and techniques currently considered to be good practices in ensuring compliance of the deceleration system with the different functional criteria.

4.1.1 Deployment and Inflation

Reliable and orderly performance of the deployment function of the deceleration system should be ensured by painstaking attention to the following critical aspects of design:

- Use of sensor, initiator, actuator, and release devices of adequate sensitivity, efficiency, and energy output
- Packaging of decelerators in appropriate-type containers with low-friction linings
- Suitable procedures, equipment, and checklists for packing and rigging
- Provisions to prevent abrasion, snagging, cutting, or impact of the deploying components on each other or on the spacecraft
- Favorable location of the storage compartment or compartments in relation to the attitude and motion of the spacecraft during flight, to the decelerator-harness attachments, and to the vehicle components that are to be jettisoned in flight

Reliable and positive inflation of decelerators should be ensured by:

- Using structural design factors that will guarantee the integrity of the envelope after it has been subjected to deployment and opening loads
- Employing proven decelerator types and proven rigging and packing methods

- Adhering carefully to design specifications governing the shape, construction, and porosity of the inflatable envelope
- Making provisions for decelerator operation at a favorable position in the wake of the vehicle
- Accounting properly for the effects of jettisoned parts such as sabot, bag covers, and other parts

4.1.2 Deceleration

Deceleration of the spacecraft in an orderly and dependable sequence should be ensured by employing:

- Decelerators having well-defined and repeatable inflation and low-shock opening characteristics
- Configurations amenable to reefed staging and having good drag-to-weight efficiency, as well as configurations free from excess transverse and longitudinal oscillations
- Efficiently designed harnesses having members of low mass and favorable energy-absorption characteristics
- Low-shock transition and staging mechanisms

4.1.3 Stabilization

Stabilization of the spacecraft after inflation of the decelerator should be ensured by:

- Employing decelerators which are themselves inherently stable
- Providing sufficiently large ratios of decelerator drag to the spacecraft mass and to aerodynamic moments
- Making the attachment-harness geometry compatible with the trim attitude of the spacecraft
- Avoiding excessive elasticity in harness and risers

4.1.4 Steady Descent

Maintaining the spacecraft descent within specified vertical- and horizontal-velocity limits should be ensured initially by a design analysis based on the recorded history of the type of decelerator under design consideration, as well as on dependable design and test data. Ultimately, however, steady-descent performance should be verified by aerial drop tests of models of the new system.

Design of decelerators to meet steady-descent performance requirements should allow for probable future growth in spacecraft weight.

4.1.5 Response to Control Signals

Good response of the deceleration system to control signals should be obtained by (1) designing control deflection into those portions of the lifting surface (tips and trailing edges) which have large-moment arms from the gravity axis or the maximum effects on the camber and twist of the lifting surface; (2) utilizing control lines of minimum elasticity; and (3) having rapid control travel.

Minimum lag and undamped oscillations in the response of the suspended vehicle to control-induced motions of the lifting surface should be achieved by (1) employing widely spaced harness attachments; (2) using harness and line materials of minimum elasticity (e.g., steel cables in series with textile materials); and (3) limiting pitch-and-turn angular accelerations to levels compatible with the elasticity of the coupling between vehicle and lifting surface.

4.1.6 Aerial-Recovery Engagement and Towing

Adequate structural integrity for engagement and towing of the recovery parachute by the aerial-pickup system should be ensured by (1) providing large design factors to compensate for anticipated nonuniform loading; (2) using interwoven canopy reinforcements treated with a friction-reducing coating; and (3) having carefully spliced load-transfer structures from the pickup-target crown to the main-canopy harness on the vehicle.

4.1.7 Terminal Deceleration and Touchdown

The termination of a satisfactory descent in a safe landing should be ensured by integrating the design of the decelerator with landing-gear design. This is best accomplished by performing a tradeoff study to establish the design-descent velocity required to minimize both the impact shocks and the combined weight of decelerator and landing gear. Landing-gear tolerances for impact velocity, wind drift, and angular deflections should be used as design constraints on the decelerator system. For example, with steerable gliding systems, drift effects can be reduced through wind penetration, and requirements for impact attenuation can be minimized by employing a decelerator capable of performing a flared-landing maneuver, as done in a deployable wing or controllable autorotor system.

4.1.8 Termination

Satisfactory separation of either a drogue stage or the main-descent surface should be ensured by employing release hardware having a minimum reaction time and the

capability of effecting synchronous release of multiple attachments. For manned systems, due regard should be given safety considerations for manual initiation of the disconnect function.

4.2 Design Characteristics

Preliminary design of a deployable aerodynamic decelerator system should be supported and validated by the process of selecting and designing the components of the system in some detail. An initial step in this process should be to make sure that the deployable aerodynamic deceleration system selected is wholly compatible with the configuration and the mission of the spacecraft. A comprehensive analysis such as that indicated in table III, which lends to charting the operational requirements underlying the detail design, is recommended. This analysis should include preliminary quantitative evaluation of the spacecraft- and decelerator-system designs. If optimization of spacecraft-decelerator-system design is desired, the optimization should be carried out in parametric form.

Potential design problems should be identified by evaluating the scope of previous development of the decelerator type under consideration in terms of whether or not system details have been assessed with respect to specific mission demands and constraints. This evaluation should then serve as a basis for defining the scope of the development-test program. The tendency to overcomplicate the decelerator system beyond actual mission constraints should be resisted as strongly as the tendency to oversimplify.

Full consideration should be given to the inherent capability of the spacecraft configuration for performance of deceleration-stabilization and controlled-descent functions when it is advisable to ensure the ultimate simplicity of the deployable decelerator, even to the point where the deployable system may serve only as an austere backup or reserve system.

In addition to the more basic and obvious aerodynamic characteristics of the decelerator, it is recommended that more complex aerodynamic characteristics such as those enumerated in Section 3.2 be evaluated. Among these are the size-limiting scale effects noted in Section 2.2.1.6. For example, an anomalous scale effect can reduce the critical opening velocity of porous, shaped canopies as size increases, which in turn increases the tendency of the canopy to squid during inflation. The limiting case is a model too large to inflate properly at moderate flight speeds. Another scale effect arises from the clustering of parachute canopies. Clustering reduces the effective-drag coefficient and, because of nonuniform opening and load sharing, leads to a substantial increase in the design-limit load of each parachute. The designer should also recognize that the use of a large, attached pilot chute on a main canopy may radically alter opening characteristics, so that load predictions cannot be based on data obtained from tests of the parachute performed without an attached pilot chute.

TABLE III—DECELERATION-SYSTEM OPERATIONAL ANALYSIS

Decelerator event	Environmental characteristics	Design considerations
Manufacture	Air temperature and humidity; cleanliness	Quality of materials; finished dimensions; dimensional tolerances
Transportation and storage	Air temperature and humidity; fungus	Shipping container; vacuum packing; repack cycle
Installation in spacecraft	Handling by man; sterilization	Pressure packing; human effects
Prelaunch checkout	Moisture and chemical leakage	Sensors; actuators; protective covering
Launch and staging	Heat, noise, shock, vibration; decreasing air pressure	Venting outward; set-back loads; thermal protection
Space journey	Vacuum; radiation; temperature	Outgassing; material degradation; spacecraft emissions
Atmospheric entry	Deceleration; dynamic heating; increasing air pressure	Inertial loads; thermal protection; venting inward
Sensor operation	Atmosphere of earth or other planet	Composition; density/altitude profile
Decelerator deployment	Dynamic pressure; shock; vibration	Ejection and snatch loads; internal friction-contact abrasion
Inflation and deceleration	Dynamic pressure; heating	Opening loads; staging and reefing; stability
Controlled descent	Wind shear and gusts; jettisoned chemicals	Jettisoned components; stability and control
Landing approach	Wind drift; topography; obstacles	Deceleration/vehicle stability and maneuverability
Touchdown	Surface gravity; slope; roughness	Impact attenuation; resistance to overturn; flotation
Termination	Surface of earth and other planet	Disconnect and separation

The designer should seek to avoid particular deployment configurations that generate high onset shocks; such configurations include (1) those that permit an attached mass (links, swivels, packs, etc.) to acquire a large relative velocity; (2) those in which a large extraction force must be applied to a mass while the mass is in an unfavorable attitude; and (3) those that allow excessive slack in a deployment-bag bridle or in actuating lanyards for slug guns, reefing-line cutters, and other such components.

When defining optimum properties for materials in steerable systems, a compromise should be made between the elongation needed for shock attenuation and the dimensional integrity desired for stability and control (ref. 65). The present practice of using Dacron materials in place of nylon (ref. 41) has little to recommend it because differences in their elasticity are not as significant in most cases as the fact that the elongation of both is large and their hysteresis similar. Risers of nylon webbing and steel cable in series have been frequently used and can be recommended as effective. (refs. 2, 31, and 54).

Material-property constraints on the flexibility of the decelerator should be considered in design (ref. 67). The best standard materials should be used, and sufficient environmental protection should be provided for components to limit the physical degradation of these materials to an acceptable level (refs. 1 and 31). When adequate protection cannot be provided, special materials that have greater environmental resistance, such as polyurethane-coated nylon or Nomex, should be used, but only in the members or structures which are vulnerable to environmental degradation (refs. 15, 27, and 28). (Additional information on material characteristics is given in Secs. 2.2.8 and 2.2.9.)

Because textile materials vary widely in quality, constant vigilance should be given to in-process and receiving inspection to ensure detection of possible defects and substandard mechanical properties.

When the finished dimensions are critical to the fit and function of the decelerator, suitable allowance should be made in design for the anomalous ways in which fabrication of textile assemblies can alter important dimensions. The nonlinear elastic properties and the hysteresis of textiles (ref. 65) should also be considered in accounting for the dimensional changes resulting from the manner of loading, which can both augment the opening shock and affect the flying trim and controllability of the main-descent surface. In overload tests, growth of the canopy to a larger-than-design drag area caused by material elongation should be allowed for.

While there appears to be no sharp upper limit to the packing density of textile assemblies, short of the solid state of the material, the designer should avoid high-density packing because of possible damage to the fabric structure or to crushable components such as reefing rings and line cutters. Moreover, damage is often difficult to detect, and X-ray inspection of each finished high-density pack is usually required.

A design-pack density of up to 505 to 560 kg/m³ (31 to 35 lb/ft³) is recommended for nylon-decelerator installations in spacecraft. A 15-percent greater design-pack density is recommended for Dacron and Nomex decelerators.

Decelerator-pack extraction by pilot chute and the impulsive ejection by mortar, catapult, or other means are attended by severe inertial and friction loads that should be accounted for in design. Use of high-density packs is recommended to minimize inertial effects. It is also desirable to minimize the possibility of abrasion and friction damage in impulsive extraction or ejection by using a low-friction material such as Teflon fabric as a lining in deployment bags. In addition, deployment bags designed for extraction by an attached bridle should have strong retainers for canopy and suspension lines to prevent disorganization or premature dumping of the decelerator.

The use of extraction devices (e.g., pilot chutes, rockets, and slug guns) instead of ejectors should be considered since decelerator-pack ejectors are relatively heavy and may impose an excessive reaction load on the spacecraft. Use of the slug gun should be limited to extracting devices with small masses, such as a pilot chute. Recommended techniques for the selection and analysis of parachute deployment systems for spacecraft are given in reference 84.

Precedence in allocating the location(s), shape(s), and volume(s) of storage space to the deceleration system should be determined by deployment requirements. The fact that available stowage volume and the configuration of the available stowage space may require the use of clustered decelerators in place of single large components should be considered. Decelerator design should be compromised as little as possible by spacecraft constraints on harness attachment and the installation of other spacecraft components. When possible, a regular-shaped compartment should be used to minimize pressure-packing problems and unfavorable dynamic effects during deployment.

Stabilization requirements during deployment and deceleration, and landing requirements during steady descent, should govern the number, type, and location of deceleration-system attachments on the vehicle. Use of a single-point attachment is recommended wherever feasible when adequate stabilization of the spacecraft can be achieved in this manner. If a transition from one spacecraft-suspension attitude to another must be made during decelerator operation, the best practice is to time this transition to occur during steady descent.

4.3 Operational Conditions

The criteria presented in Section 3.3 provide a good checklist of the operational conditions to be evaluated to support the selection and design of a deployable decelerator. The major operational conditions are the dynamic pressure, velocity, gross weight, ballistic coefficient, and motion of the spacecraft at system deployment, as well as the desired equilibrium-descent velocity at a given altitude. Analysis of loads and stresses is discussed in Section 4.6.

Launch, ascent, and staging conditions should be evaluated for any heating or acceleration transients more severe than the deployment conditions which normally "design" the decelerator system. Components which can be affected during launch include the protective cover of the deceleration-system compartment, exposed harness members, thermal insulation, and the hold-down members for packs and rigging (ref. 1). Considerations of launch, ascent, and staging, along with those of heat sterilization, are likely to have a stronger influence on the selection of a decelerator material for a Mars lander than are the operational conditions expected on that planet. Opening loads, decelerator area, staging, and drogue requirements should be defined for the normal operational modes and, for manned spacecraft, the abort modes. These data should be accumulated and formalized early in the spacecraft-design program. For termination on another planet, the best possible definition of atmospheric properties, gravitational acceleration, and surface winds should be obtained.

In most instances, atmospheric-entry conditions are expected to produce the dominant thermal effect on materials. In addition to the use of protective covers and insulation, decelerator performance in thermal environments should be provided for by using metal risers and fittings in exposed areas adjoining the structural attachment points on the exterior of the entry vehicle (refs. 1, 2, and 54). When a decelerator deploys at velocities above Mach 3, aerodynamic heating becomes significant (refs. 15, 16 and 59). Under such circumstances, allowance should be made in the system design for degradation of decelerator efficiency due both to the loss of material strength and to the use of textiles heavier than nylon (e.g., Nomex).

Degradation of material physical and mechanical properties resulting from prolonged exposure to the space environment should be evaluated by test for the duration of the proposed mission. At the present time, decelerator materials or protective measures have proven adequate for Apollo missions. There is little reason to doubt that decelerator materials could endure much longer storage in space with protection equivalent to Apollo practices.

Degradation of material physical properties from sterilization-heating cycles may be measured in the laboratory (refs. 64 and 66) and should be allowed for in structural design by applying a suitable factor to account for temperature degradation in the strengths of materials.

4.4 Design Constraints

Section 3.4 provides a checklist of minimum constraints to be considered in the selection and development of a deployable deceleration system; references 4, 7, 9, 10, 41, and 44 provide supplementary details.

When using reefing to limit peak opening loads and accelerations on circular canopies, the standard radial-skirt method, with rings at each suspension-line attachment, is

preferable to the midgore method with rings attached to the skirt on the center line of each gore because more documented experience is available to guide analysis. The effectiveness of midgore reefing depends somewhat on the type of canopy with which it is used. On the other hand, midgore reefing improves the stability of the inlet area of asymmetrically ventilated canopies and, in steady flow, of circular canopies. It was employed on the Apollo parachute system (refs. 1 and 31) because it was believed to afford certain advantages over radial reefing. However, under dynamic-opening conditions, the only difference discernible in flight tests is that midgore reefing produces a somewhat greater drag area for a given reefing ratio, as shown in figure 7. Midgore reefing of ribbon drogues should be avoided because it tends to neutralize the function of the pocket bands in getting canopy filling started.

Where compatible with spacecraft constraints, it is recommended that the decelerator design include allowance for the growth of spacecraft weight. If the volume allowed for the decelerator is limited, one recourse generally taken is to pressure-pack the fabric components to a relatively high density (ref. 31). (Table II in Sec. 2 gives practical limits for packing density.) A more difficult practice, but recommended for use whenever it is feasible, is to optimize decelerator design for the specific application. In such instances, it is desirable to initiate the optimization program by considering the tradeoffs possible between different approaches toward meeting basic decelerator functions. For example, there is an optimum design sinking speed at touchdown for each combination of main-descent system and landing device (such as parachutes and retrorockets) which should be evaluated. Also, where applicable, the relative sizes of the drogue and main decelerator should be optimized for a system of minimum weight.

When the maximum equilibrium-descent velocity is a firm requirement, it is advisable to use a 2σ or 3σ smaller design value for this velocity to allow for the normal variation in the rate of descent encountered in actual operation. An alternative practice, more commonly used, is to base decelerator design on average descent rates and include normal variations in descent rates as part of the inputs for designing the landing gear or impact- and velocity-attenuation systems.

The design of an aerial-recovery system of the type used for instrumented entry capsules can be facilitated by several practices. Spacecraft-weight variation should be defined within the narrowest possible limits, while at the same time system-stability and rate-of-descent performance requirements should be liberalized as much as possible. The rate of descent presently recommended for design is 7.6 m/sec (25 fps) at a 3-km (10 000-ft) altitude. Since an aerial-recovery decelerator must inflate reliably at an altitude of 13.7 to 15.2 km (45 000 to 50 000 ft), the high shock-loading condition caused by deployment at these altitudes should be given particular attention in both functional and structural aspects of the design (refs. 3 and 4). The known limitations of present aerial-recovery systems should be accounted for in current design.

Stability requirements for descent and landing should be made as liberal as possible since unnecessary restrictions can limit freedom of choice in selecting the type of

main-descent surface. Pendular or coning oscillations of 10 to 15 degrees from the vertical generally have no adverse effects on an unmanned payload; however, the effects of the amplitude and frequency of the oscillations on a spacecraft crew should be considered.

When parts of the spacecraft are to be jettisoned during the operation of the deployable deceleration system, the component mass, method of release, and flight conditions at the time of the jettison should be evaluated for their effect on decelerator-system deployment, opening loads, structural integrity, and descent characteristics.

The specific conditions under which deceleration-system operation is to be terminated (e.g., time, altitude, loading, or velocity) should also be clearly defined so that the termination control and actuator components can be designed to operate safely.

Manufacture should be facilitated by various practices, such as (1) providing extensive fabrication on the subassembly level of sails, gores, and sections to minimize the amount of detail work during final assembly; (2) limiting seam thicknesses and tape plies to the capacity of standard sewing machines; (3) avoiding the specification of unnecessarily tight dimensional tolerances; and (4) avoiding specifications to finish to the design dimensions when such specifications serve no useful purpose (as is usually the case since the decelerator is stretched to larger-than-design size in all dimensions under design-loading conditions). On the other hand, where cloth gathering and shrinkage along seams are not acceptable, as in textile assemblies that must fit rigid parts, it is necessary to specify finishing to the design dimensions so that a suitable shrink scale will be employed when material is laid out for cutting.

Generally, the designer should have a good working knowledge of textile design, spinning, weaving, and processing to ensure the proper interface between design and manufacture of decelerator structures. While virtually any fabric shape can be assembled by present methods, manufacture and quality control, as well as packing and rigging, should be facilitated by taking the precautions during preliminary design to preclude unessential complication of the decelerator assembly, stowage-compartment shape, and method of deployment.

Communication, location, and retrieval devices on the capsule may sometimes influence the design of the deployable deceleration system and, even though this influence may be minor, it should be accounted for. The decelerator should be designed to permit such devices to be activated or erected during descent through the atmosphere, when necessary, and to continue to function after touchdown and the disconnect of the main-decelerator surface. It is also good practice to use the decelerator itself as a location aid by making it of bright-colored fabric.

Uniformity and interchangeability of decelerator components should be ensured by specifying the tensions to be applied when both materials and the finished assembly are

measured, and by specifying suitable tolerances for all finished dimensions critical to decelerator performance. In a parachute, for example, suitable tolerances should be specified for the lengths of suspension lines and radial seams and for gore widths at skirt and vent. Because of the effects of natural and induced environments on deployable-decelerator structures and the cost of inspection and recertification, refurbishment and reuse are seldom, if ever, specified for spacecraft application; accordingly, design for reuse is not presently recommended.

Ground-handling safety requirements for deployable decelerators are readily satisfied on the level of design through observance of certain recommended precautionary practices, such as (1) using arming pins in the reefing-line cutters and shorting bridges in deployment-gun and mortar cartridges; (2) loading cartridges through the breeches rather than through the muzzles of thrusters, catapults, and mortars; (3) avoiding devices employing strong springs in the cocked position; and (4) using nonreactive outlets on high-pressure gas reservoirs. All safety regulations and procedures for the handling of explosive devices should be strictly observed.

Safety during operation of the deceleration system should be ensured by special precautions, including (1) adequate amperage requirements for no-fire and all-fire of pyroelectric initiators; (2) locked-cover tests for mortars to demonstrate structural integrity of both breech and barrel; (3) arming of inertia switches during steady descent (after all peak-load and impact transients have occurred); and (4) providing protective covers for manual override switches used for initiation of deployment and disconnect operations.

Established reliability-design practices should be used to ensure the functioning of decelerators. These practices require provisions for (1) redundant sensor and initiator circuits; (2) sympathetic firing of independently initiated dual-mortar cartridges; (3) reserve power supplies; and (4) redundancy of independently deployed decelerators (both drogue and main surfaces).

Structural reliability should be ensured by (1) determining the probable effects of variations in component performance, including failures of single components, on maximum applied loads; (2) using a suitable design factor to establish the ultimate load; and (3) performing tests that demonstrate structural integrity under the critical loading conditions for each operational stage of the drogue and main decelerators.

4.5 Selection

A value matrix is recommended for comparison of candidate deployable deceleration systems. This matrix should include factors pertinent to the specific spacecraft mission, similar to those listed in Section 2.3. Tables IV and V are examples of comparison matrixes that have been used to guide the selection of a manned-spacecraft landing system and an aerial-recovery system. Specific value judgments given in the examples

TABLE IV. -- COMPARISON OF LAND-LANDING SYSTEMS FOR A MANNED
SPACECRAFT (Ref. 85)

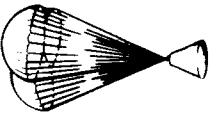
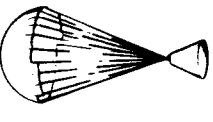
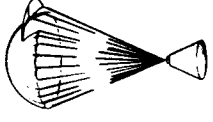
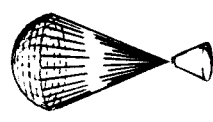
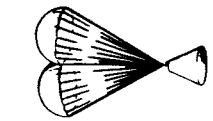


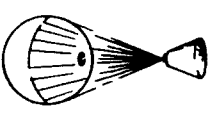
System	Cloverleaf steerable parachute, $L/D = 0.8$ to 1.8	Parasail, $L/D = 1.1$	Glidesail, $L/D = 0.6$, cluster of 3	Ringsail, $L/D = 0$, cluster of 3	Small stabilizing parachute (no main chute)	Paraglider	Rotors	Paravulcoon
Characteristics								
Deployment	Fair High opening loads; may require two-stage reefing	Fair Large chute	Fair Multiple-chute deployment	Fair Multiple-chute deployment	Good Simple parachute deployment	Poor Severe deployment	Poor Bulky and complex	Poor Bulky and complex
Complexity and reliability	Poor Complex control system required	Fair Complex control system	Fair Complex control system	Good Simple	Good Simple, reliable system.	Poor Complex deployment and control problems	Poor Antitarget device required	Poor Potential fire or explosion hazard
Parachute weight per unit radius/surface area	Good High L/D allows small chute diameter	Poor Large-diameter, low-porosity parachute	Fair Lighter than ring-sail	Fair Low C_D and zero lift result in large-diameter	Good Lightest descent system possible	Poor Heavier than gliding parachutes	Poor Extremely heavy system	Poor Heavier than gliding parachute
Wind cancellation	Good Good L/D range	Fair Good L/D but not variable	Fair Low L/D	Poor None	Poor None	Good High $L/D = 2.5$; partial flare capability	Good Excellent L/D	Poor No steering capability

TABLE IV. -- COMPARISON OF LAND-LANDING SYSTEMS FOR A MANNED SPACECRAFT (Ref. 85) -- Concluded

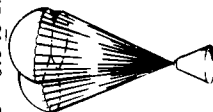
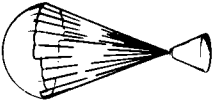
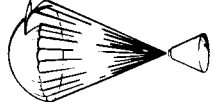
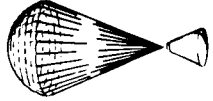
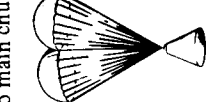


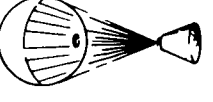
System Characteristics	Cloverleaf steerable parachute, $L/D = 0.8$ to 1.8	Parasail, $L/D = 1.1$	Glidesail, $L/D = 0.6$, cluster of 3	Ringsail $L/D = 0$, cluster of 3	Small stabilizing parachute (no main chute)	Paraglider	Rotors	Paravulcocon
								
Maneuver capability	Good	Good	Fair	Poor	Poor	Good	Good	Fair
	High L/D ratio; fast response	Good L/D ; fair response	Slow response; low L/D	None	None	Good turn rate and fair stability	Excellent maneuver capability and rate-of-descent control	Low rate of descent but no maneuver capability
Self backup capability	Poor	Poor	Good	Good	Good	Poor	Poor	Good
	Separate backup system required	Separate backup system required	Can be clustered for redundancy	Can be clustered for redundancy	Redundant drogue; can be clustered	Requires auxiliary system	Requires auxiliary system	Cluster system provides redundancy
Development	Poor	Fair	Fair	Good	Good	Poor	Poor	Fair
	Preliminary stages; small chutes	Advanced stages	Well developed	Well developed; large chutes	Well-tested system	Extensive development effort required for deployment and stability	Extensive development required for stowage and deployment	Partial development on smaller scale
General comment	Selected system; adequate time needed for development		Could be best system with a good overturn- stability device		Must be used with a large rocket braking system and with an overturn- prevention device	Rejected because of severe deployment problems; potential for future applications	Requires much development effort	No specific advantage not provided by other systems

TABLE V.—EXAMPLE OF A COMPARISON MATRIX FOR A UNIVERSAL AERIAL-RECOVERY SYSTEM (Ref. 31)

Characteristic	System Designation						
	A Tandem	B Cone	C Glidesail	D Ringsail	E-1 Annular	E-2 Annular	E-3 Annular
Drag efficiency ($\Sigma C_D S/W$) m ² /kg (ft ² /lb)	4.7 ≈(23)	47.7 (19.4-37.8)	6.4-10.9 (31.6-53.3)	4.3-8.2 (21-40)	50% V. 5.1-9.2 (25-45)	65% V. 5.1-9.3 (25-46)	80% V. 5.1-9.0 (25-44)
Stability	Poor	Good	Good	Fair	Fair	Good	Fair
Deployment and opening	Fair	Fair	Poor	Good	Fair	Fair	Fair
Reinflation reliability	Fair	Good	Poor	Good	Fair	Good	Good
Pickup target resistance to collapse after damage	Fair	Fair	Poor	Fair	Good	Good	Good
Uniformity of pickup loads	Good	Fair	Poor	Fair	Fair	Fair	Fair
Reliability of engagement	Fair	Good	Poor	Good	Good	Good	Good
Main canopy reel-in behavior	Good	Fair	Fair	Good	Fair	Fair	Fair
Initial contact behavior	Good	Good	Fair	Good	Good	Good	Good
Compatibility with engagement	Good	Good	Poor	Good	Good	Good	Good
Visual acquisition	Good	Good	Fair	Good	Good	Good	Good
Scaling characteristics	Good	Good	Fair	Good	Good	Good	Good
Reefing simplicity	Fair	Fair	Poor	Fair	Fair	Good	Good
Economy of fabrication	Fair	Good	Fair	Fair	Good	Good	Good
Reinflation ability of main	Good	Good	Good	Good	Good	Good	Good
Ease of rigging and packing	Fair	Fair	Fair	Good	Poor	Poor	Poor
Scoring:							
Numerical drag efficiency rating	23	30	42.5	30.5	35	36	34.5
No. of "Good" ratings (x 3)	(7) 21	(9) 27	(3) 9	(10) 30	(8) 24	(11) 33	(10) 30
No. of "Fair" ratings (x 2)	(7) 14	(6) 12	(5) 10	(5) 10	(6) 12	(3) 6	(4) 8
No. of "Poor" ratings (x 1)	(1) 1	(0) 0	(7) 7	(0) 0	(1) 1	(1) 1	(1) 1
Totals	59	69	68.5	70.5	72	76	73.5

are not necessarily applicable to new system designs. Where sophisticated spacecraft and space-mission concepts are involved, comparative testing of two or more candidate systems to fill gaps in the existing knowledge is recommended before a selection of a decelerator type is made.

The use of new or of novel decelerators should be carefully appraised, and if a novel approach is selected, a well-qualified alternate should be developed in parallel until the new decelerator is fully qualified. Moreover, the selection of a deployable aerodynamic deceleration system for a specific spacecraft should be validated by a comprehensive program of load verification, qualification, and acceptance testing even if well-developed components are used.

Where an equivalent single parachute will meet requirements, parachute clusters should be avoided in ballistic systems because a cluster does not open uniformly and has a lower drag-to-weight efficiency (~ 15 percent less for a three-canopy cluster). Tandem canopies (two canopies in series, with one operating in the wake of the other) should be avoided for similar reasons. The advantages and disadvantages of using a pilot chute that is permanently attached to the apex of the main canopy should be carefully weighed for each specific application. On the affirmative side, such a pilot chute prevents whipping of the main-canopy apex during the initial filling stage and, when relatively large (~ 3 percent of the main-canopy drag surface), the pilot chute will retard the filling and reduce the opening load of the main canopy. On the negative side, use of the attached pilot chute may necessitate supplementary drop tests for load verification because it modifies the opening characteristics of the main canopy in ways that have not been quantitatively evaluated for many conditions.

A single canopy, up to the largest size compatible with operationally qualified recovery gear, is recommended for the aerial recovery of entry capsules. Where larger parachutes are required, a number of alternatives should be evaluated, including the older tandem system and the recently developed annular and conical-extension parachute systems described in references 3, 5, and 6.

Use of steerable gliding-parachute and deployable-wing systems should be evaluated on the basis of realistic operational requirements for gliding because the system weight tends to be directly proportional to maximum L/D . Moreover, weight can be doubled if reliability dictates a duplicate backup system. Maneuverability supplied by a decelerator can be traded off in design, with provisions by other spacecraft systems for precise entry or with ground-operations capability to recover a capsule over a wide landing area. However, even under conditions of precise-entry or wide-area-recovery capability, the gliding-parachute system merits consideration because it can reduce landing-impact loads, and the consequent saving in weight in spacecraft structure may more than offset the weight increase of the parachute. The advantages of employing landing rockets to decrease touchdown loads should also be considered, particularly when small structural load factors are desired in the spacecraft.

4.6 Design Analysis

When making a design analysis, the size of the main decelerator should be calculated first since it is basic to subsequent component- and system-design calculations. A generally satisfactory practice in determining the area of the main surface is to assume steady-state conditions and to set the vertical component of the aerodynamic force equal to the gross weight of the system; that is, the small effects of vehicle drag and increasing atmospheric density during steady descent can be neglected.

When unsteady conditions exist, as during deployment, opening, or rapid descent, the basic equations of motion for a point-mass system with at least two degrees of freedom should be used to provide satisfactory descriptions of the trajectory. In this approach, system-drag area is treated as a step-function of time, as described in reference 7. However, calculating decelerator-opening forces within useful tolerances requires another approach which takes into account the momentum and inertial effects of the added air mass, as discussed in Section 4.6.2.

4.6.1 Decelerator Aerodynamic Performance

Calculation of decelerator performance for design purposes depends upon the existence of empirical data of the kinds shown schematically in figures 2, 4, 5, and 7. In parachutes, the interdependence of drag coefficient, stability, and opening-load factor, indicated by the effects of canopy porosity and shape parameters, requires a compromise between drag/weight efficiency and the amplitude of characteristic oscillations. Each type of parachute listed in table I represents a different compromise, and it is a common practice to select the type having acceptable stability and the highest drag efficiency ($C_D S/W_p$), in combination with other desirable qualities such as low opening shock or strong opening tendency. When the unit-canopy loading is greater than approximately 38.3 N/m^2 (0.8 psf), use of a ventilated annulate canopy (the ringsail, for example) is recommended because the drag coefficient of this type of decelerator remains constant with increased loading.

Data on the variation of drag coefficient with suspension-line length (fig. 2b) should be used for a specific application to calculate line lengths for which the weight of the parachute will be minimum. In drogue chutes, the use of long lines is recommended to counter the loss of efficiency due to wake effects. Since drogue drag in the vehicle wake varies directly with trailing distance over a wide range of trailing distances, a tradeoff study should be made to determine the riser lengths for a minimum-weight assembly. Line lengths up to a maximum of about two drogue diameters may be considered in the tradeoff study.

When selecting a particular type of parachute for the deceleration system, it should be recognized that the filling time, an important factor related to both opening shock and reliability considerations, becomes protracted and erratic with increasing canopy size in canopies which have either a high relative porosity or an inverted conical skirt. To

avoid problems caused by erratic filling, annulate canopies of the ribbon and ringslot types should be equipped both with pocket bands across the line joints at the skirt and the correct number of vertical tapes across the slots. The slow, erratic filling of a canopy having an inverted conical skirt can be corrected either by added pocket bands or by a design change increasing the angle of attack of the skirt. When a short filling time is desired, a canopy design should be selected which has (1) a lower-than-normal porosity, (2) a flared skirt (i.e., shaped like a bellmouth), or (3) a cascade of sails operating at a high angle of attack, as in the ringsail.

Use of the dimensionless filling interval, K_f , determined by full-scale drop tests, is recommended to simplify calculation of the filling distance in trajectory studies for abort modes where altitude loss is a critical factor. The filling distance tends to be a constant, irrespective of altitude, for a given parachute configuration over a broad range of subsonic speeds. The fact that this rule cannot be applied at very low speeds nor at supersonic speeds should be allowed for in the analyses. The effect of compressibility on parachute-opening distance and filling time can be estimated as shown in reference 73.

While the dependence of deployable-wing performance on configuration parameters, such as aspect ratio, sweepback, leading-edge-shape camber, tip deflection, and other parameters, is well established for wind-tunnel models, methods for calculating aerodynamic performance of operational deployable wings cannot be recommended because the scaling laws have not been adequately defined in all cases (ref. 13). By the same token, methods for calculating the performance of the steerable parachute cannot be recommended since the steerable parachute has the characteristics of a deployable wing of small L/D , as well as those of a ballistic parachute.

For preliminary design purposes, satisfactory weight estimates can be made for parachutes with the aid of published engineering data curves for specific structural classes (light, medium, and heavy). However, this method is not accurate enough for detail design nor for decelerator-efficiency comparisons; the decelerator design must be defined in sufficient detail to establish the dimensions and materials of all components.

Unit weights of materials can be found in documents such as references 7 and 86. Reference 86 is especially useful since it contains summarized and consolidated information extracted from WADD Technical Reports covering several phases of fibrous-materials research, and is arranged to make this information readily available and directly applicable to decelerator design.

The weight and drag-to-weight efficiency ($C_D S/W_p$) of the decelerator assembly can be calculated with good accuracy using available unit-weight data for textiles. For lifting decelerators, similarly, the lift-to-weight efficiency ($C_L S/W_w$) at a given ratio of L/D

can be calculated accurately from textile unit-weight data. A more generally valid method of measuring the merit of decelerators is developed in reference 87 and presented as graphs of the ratio of weight to drag area (W_P/C_{DS}) versus dynamic pressure times the square root of drag area [$q(C_{DS})^{1/2}$].

4.6.2 Opening Loads

The opening-load-factor method, described in references 4, 7, 34, 35, and 41, is recommended for predicting opening loads for both parachutes and deployable wings. Despite its severe limitations, dependable results can be obtained when this method is carefully applied, as discussed in Section 2.2.1. If the required empirical data are unavailable, suitable tests should be performed (ref. 11). Given dependable data on the variation of the opening-load factor, C_K , with mass ratio, R_m , for the decelerator configuration of interest (either nonreefed, reefed, or disreefed), the opening force, F_O , should be calculated from the relationship:

$$F_O = \psi q_1 C_K \quad (1)$$

where ψ is the effective drag area at the end of the filling process and q_1 is the dynamic pressure at the start of filling (e.g., at line stretch). C_K should be read from a data graph like that presented as figure 2f, at the value of the mass ratio calculated from the relationship:

$$R_m = \frac{\rho \psi^{3/2}}{M} \quad (2)$$

where ρ is the air density at the deployment altitude and M is the lumped mass of spacecraft and decelerator.

Application of the foregoing method for predicting opening loads for the final filling stage for clustered parachutes after disreefing is demonstrated in reference 71. In this instance, C_K should be determined from empirical data curves relating the weight-to-drag ratio, W/C_{DS} , and the equivalent air speed at line stretch (corresponding to q_1) to other parameters which account for the effect of nonsynchronous disreefing and the portion of the total weight carried by each canopy. The opening-load-factor method can potentially predict loads to within an accuracy of approximately 10 percent.

The alternate mass-time method for predicting opening loads, which employs a digital-computer program, is recommended when accuracy on the order of ± 5 percent is desired and sufficient data are available from three or four drop tests to quantify such parachute parameters as (1) the full-open drag area and the drag areas at the beginning and end of each reefed stage; (2) the order of the differential equation describing the time growth of the drag area, which in the final filling stage is a function of the filling time; and (3) the dimensionless filling time defined as:

$$K_f = \frac{\Delta t_f v_1}{\psi_2^{1/2} - \psi_1^{1/2}} \quad (3)$$

where Δt_f is the filling time of the canopy while growing from its initial drag area ψ_1 to its final drag area ψ_2 , and v_1 is the true airspeed at the start of the filling interval. The relationship of the shape factor of the parachute, K_a , to the added air mass, m_a , should be included in the calculation, as defined by the expression:

$$K_a = \frac{m_a}{\rho \psi^{3/2}} \quad (4)$$

Necessary definitions of the mass-time method parameters should be derived from test data by using the computer program described in reference 70.

When the opening force is modulated by riser pulsations caused by oscillation of the spacecraft, the method of calculation illustrated in reference 79 (as discussed in Sec. 2.4) is recommended.

4.6.3 Deployment (Snatch) Forces and Reaction Loads

The recommended method of predicting snatch force is to use a digital-computer program describing a two-body spring-mass system to calculate a time history of undamped spring deflection and the resultant spring tension; that is, the snatch force in the decelerator riser.

When it is feasible to neglect drag and treat the connecting member (riser plus lines) as a linear spring, a preliminary approximation of the maximum snatch force, F_s , may be made from the expression:

$$F_s = \Delta v (Km)^{1/2} \quad (5)$$

where Δv is the velocity differential between vehicle and decelerator pack at line stretch, K is the effective spring constant, and m is the mass of the pack plus one third of the mass of the riser and lines.

The drag of the attached pilot chute should not be neglected in calculating the impact or reaction load experienced at the end of deployment, when the main canopy comes taut and the fully inflated pilot chute is impulsively reaccelerated to the vehicle velocity. The digital-computer method recommended for calculating snatch force can be used for calculating this impact. However, results should be used circumspectly because the computed load will not be conservative when the shock onset is sufficiently high to generate traveling stress waves in the pilot-chute riser. This phenomenon is fairly well understood (refs. 14 and 72), but methods of coping with it

analytically have not been developed to a level of usefulness.

The mortar-reaction load attending deployment of a pilot chute, drogue, or main decelerator may be calculated by standard methods based on Newton's third law, when the internal ballistics of the mortar are known. Usually, test data on internal pressure versus time, or the ratio of peak to average pressure, are available so that both the muzzle velocity and reaction load can be predicted with reasonable accuracy for any given mass to be ejected. A method of predicting mortar-ejection velocity in flight from ground-test measurements is given in reference 84. This source also discusses the advantages of a rocket-extraction system and presents an accurate method of making weight calculations for such a system.

4.6.4 Stress Analysis

The empirical methods for stress analysis given in reference 1 and illustrated in references 4, 15, 34, and 75 are recommended for making quick evaluations of stress. These methods are derived primarily from membrane theory such as that given in reference 82. For example, the expression for the circumferential-unit load, or "hoopstress," in an ellipsoidal surface of revolution, T_C , is written as:

$$T_C = pr_C - T_2 (r_C/r_2) \quad (6)$$

where p is a uniformly distributed pressure, r_C is the local radius of curvature in the circumferential direction, T_2 is the unit load in the meridional direction, and r_2 is the local radius of curvature of the meridian.

The difficulty inherent in attempting to apply equation (6) to a decelerator surface that is not a surface of revolution is evident, although it is well suited for computing unit loads of biaxial structures like woven fabric. For convenience, the simplest form of equation (6) is used in developing empirical data; that is, $T_C = Kpr$, where K is 1.0 for simple curvature (conical, cylindrical) and 0.5 for a spherical surface. For other shapes, K falls between 0.5 and 1.0.

An acceptable alternative for making preliminary empirical evaluations of stress, used more often with parachutes, is to assume that the gross shape of the inflated canopy is spherical and to utilize test measurements to establish reasonable values for the pressure and radius of curvature in critical areas, such as the crown cloth as it bulges between radial ribs or in a circumferential band. A uniform pressure distribution can be reasonably assumed for circular canopies (refs. 4 and 34).

Once the decelerator structure has been defined in detail, the methods of references 14 and 72 should be used and will yield dependable results if the inflated shape of the canopy is adequately defined. For ballutes and attached inflatable decelerators, the isotenoid method presented in references 8 and 27 is applicable; large design factors (3

to 5) are recommended to cover the critical flagging stresses generated by fluttering and whipping during inflation.

4.6.5 Structural Design Factors

In order to conform with generally accepted practice in structural design and analysis, the approach to textile structures outlined in reference 34 should be followed in making use of the design-factor data given in reference 7, page 370. This approach applies to the following two factors:

1. A strength-reducing factor, A_p , is applied to rated or measured strength levels of fabric material to account for losses of strength caused by such known phenomena as abrasion, fatigue, environment (temperature, humidity, and vacuum), joint efficiency, nonuniform loading, line convergence, etc. Thus, A_p is the product of a series of numbers representing loss of strength resulting from various conditions, phenomena, and environments.
2. A safety factor (S.F.) is applied to the limit load to determine the ultimate load, and is intended to account for uncontrollable variations in material properties and degradations resulting from manufacturing processes. Decelerator structural elements are expected to withstand ultimate loads without failure and limit loads without permanent deformation.

The two factors should be separately defined and taken into account for each decelerator structural element.

Proper relationship of the allowable strength and applied load derived by using the foregoing factors should be ensured by means of margins of safety (M.S.) computed for each structural element of the decelerator by:

$$M.S. = \frac{1}{R} - 1 \quad (7)$$

where R is the ratio of applied load to allowable strength. Table VI presents typical safety factors for the structural elements of a circular parachute.

The allowable strength, P_A , of the material (fabric, cord, webbing) is calculated by:

$$P_A = A_p P_R \quad (8)$$

where P_R is either the minimum-rated ("spec") strength or minimum-measured strength of the material, as determined by standard testing procedures. A_p is also used to determine an overall structural design factor (D.F.) as follows:

$$D.F. = \frac{S.F.}{A_p} \quad (9)$$

where S.F. is the desired safety factor or ratio of the design ultimate load to the limit load.

For design purposes, the required minimum strength of material, P'_R , for a given member is calculated by:

$$P'_R = \frac{(D.F.) (\text{Limit Load})}{z} \quad (10)$$

where z is the number of identical cords, webs, or tape plies in the member, and is equal to unity for fabric since the use of plied fabrics is not recommended for the primary surface except where local reinforcements are needed. The material selected is usually the lightest of those having a rated strength, P_R , greater than P'_R .

In good practice, design factors range from $D.F. = 1.9$ to as much as 4 or 5. When the calculated allowable strength factor, A_p , is large, it is advisable to employ a safety factor large enough to ensure that the design factor will not be less than 1.9 to 2.0 because the element of uncertainty in textile structures subject to dynamic-loading conditions remains substantial. The use of large safety factors is justified in critical single members, the failure of which could lead to catastrophic failure of the system, but not in major decelerator structures, which ordinarily have sufficient redundancy.

It is clear that structural design factors must be carefully evaluated in order to avoid unnecessary weight penalties while meeting reliability requirements. For this reason, no blanket recommendations can be made for decelerators. The safety factors given in table VI for circular parachutes are representative of good current practice.

TABLE VI. – CIRCULAR-PARACHUTE SAFETY FACTORS

Component	Safety factor
Drogue canopy	1.5
Main canopy	1.35 to 1.5
Suspension line	1.5
Risers	2.0
Metal parts	1.25 to 1.5

4.6.6 Deceleration Staging

Whether or not more than one deceleration stage is needed can be quickly established by estimation of the opening load of the main surface (nonreefed), with the assumption that it is deployed at the specified altitude, flight-path angle, and dynamic pressure (or Mach number). A series of trial calculations should be made to determine the probable number of reefed stages and/or drogue stages required to hold peak loads below the allowable limits for the spacecraft structure, payload, or crew. Whenever feasible, it is desirable to limit the number of reefed stages to one per main surface. However, a need for a high unit-canopy loading or low-porosity fabric in the main surface can make additional reefed stages mandatory. For example, the Apollo earth-landing system has one reefed stage in the drogues and two in each main parachute, while large deployable wings require four or more reefed stages.

A good practice in the determination of reefing parameters (e.g., diameter ratio and reefing time) is to provide for equal peak loads in each stage at the critical design-deployment conditions. Equalization of drogue and main-decelerator peak loads may also be desirable for uniformity of deceleration, but is not always feasible because of differences in the provisions for transmission and distribution of loads in the spacecraft structure.

4.6.7 Aerodynamic Stability

To ensure the elimination of each instability mode during deceleration, descent, and landing operations that is inconsistent with spacecraft mission constraints, calculations of the following stability conditions should be made as required:

- Static and dynamic stability of the system as a whole
- Relative amplitude of pitch, yaw, and roll oscillations between the decelerator and the spacecraft
- Amplitude and frequency of both transverse and longitudinal oscillations

Theoretical treatment of various aspects of decelerator stability can be found in references 7, 74, and 80. Standard analytical methods providing for three to six degrees of freedom are acceptable where adequate empirical data exist; however, in most cases carefully designed tests should also be performed.

4.6.8 Wake Effects

The effects of wake on decelerator performance should be taken into account in design. These effects can be calculated from empirical data on the variation in drag coefficient of trailing surfaces of different types in the wake of bodies of different

shapes as the relative size and relative trailing distance are varied (e.g., fig. 4). In addition, an analytical method for approximating the body wake and its effect on decelerator performance has been developed (refs. 29 and 57), and a reasonable correlation of effects predicted by this method and experimental results have been obtained. Other data applicable to wake-effect calculation are given in references 7, 48, and 56.

4.6.9 Dynamic-Heating Effects

Degradation of structural strength by the dynamic heating of decelerators deployed at high Mach numbers and dynamic pressure should be allowed for in design. Such dynamic-heating effects on decelerator materials may be estimated by the methods given in references 7, 27, and 47, and illustrated by examples for both ribbon drogues and ballutes in references 15 and 27. Test data on the measured thermal properties of materials should be obtained to calculate the probable temperature rise when the critical members of the structure are subjected to a transient heat flux in the wake of the towing vehicle.

4.6.10 Aerodynamic Performance of Deployable Wings

There are no suitable methods for calculating the control and stability characteristics of deployable wings, except on the basis of adequate empirical data directly applicable to the particular system under design. For manned spacecraft, prediction of the relative motion of deployable wing and capsule throughout the descent as a guide for design of spacecraft suspension, harnessing structure, and control is especially desirable since the onboard pilot without GCA (Ground Control Approach) depends strongly on dynamic stability to achieve the proper maneuvers.

4.6.11 Reliability

Component- and system-reliability calculations should be performed by standard methods based on the estimated or observed failure rate of each member in the operational loop to guide various design decisions (such as the type of redundancy to be employed in the main sequence). The recommended approach to system-reliability calculations is illustrated in reference 31.

4.7 Tests

It is recommended that a sufficient number of tests for design development, load verification, qualification, and acceptance be planned to assure a realistic evaluation of the performance and reliability of the deceleration system and its components. Particular attention should be given to the inspection and testing of textiles for the detection of possible defects and substandard mechanical properties.

Suitable design-development tests should be performed to verify the evaluation of all component and system parameters of deployable decelerators when evaluation by analytical methods may lead to uncertain conclusions. A large number of tests should be performed because the complexity of decelerator operation precludes accurate prediction of performance in all but the most rudimentary sense. Moreover, where small-model test results are subject to undefined scaling laws, the designer should rely only on full-scale tests.

Before any full-scale, instrumented drop test is performed, it is good practice to perform a functional drop test in which the capsule is simulated by a low-cost vehicle or by weight bomb.

For evaluating performance in wind-tunnel and free-flight tests, it is generally advisable to use test specimens that are rugged enough to ensure that structural damage that could cast doubt on the validity of the results does not occur; for example, a split gore on opening invalidates opening load, rate of descent, and stability measurements by augmenting the geometric porosity of the canopy. If fragile test specimens must be used during performance evaluation in aerial drops, then the test conditions should be moderated as much as possible to avoid invalidating the test because of damage.

Deceleration loads should be verified and systems should be qualified by aerial-drop tests which demonstrate decelerator-system structural integrity under conditions more severe than anticipated (ideally, under ultimate load). In these tests, the design-operational conditions of velocity and dynamic pressure at each stage in the deceleration process where a significant peak load occurs should be simulated as realistically as possible. Fully realistic simulation is difficult, partly because current testing techniques and instrumentation characteristically produce peak-load data with a dispersion of approximately ± 10 percent. Care in the selection of test methods and instrumentation techniques can add to the precision of test performance and results, and such care should be exercised.

The designer should be aware of the particular advantages and limitations of several approaches to a drop-test demonstration of structural capability at overdesign conditions which are available and have been used in prior programs. Drop tests can be controlled to subject the decelerator to (1) overdesign velocity or dynamic pressure, (2) overdesign weight, (3) overdesign opening load, or (4) some combination of (1), (2), and (3). The only practical method of producing an overload under "infinite-mass" conditions (i.e., conditions during the inflation experienced under relatively constant velocity) is to subject the decelerator to overdesign velocity or dynamic pressure. The advantages and limitations of the various approaches for producing overloads under "finite-mass" conditions (i.e., where a significant velocity change occurs during inflation) can be summarized as follows:

- Overdesign velocity or dynamic pressure will produce higher initial loads and higher stress in the first portion of the canopy to develop, and, if carried to

extreme, possibly unrepresentative flutter problems or aeroelastic/dynamic loading problems for certain elements of the decelerator. Increased velocity or dynamic pressure alters the conditions of deployment. The loads induced by testing at overdesign velocity are initially attenuated by finite-mass inflation, and the system is not subject to the proper overload condition through later stages of inflation. For this reason, each reefed stage should be tested separately under overdesign-velocity conditions.

- Overdesign weight, by causing a slower deceleration, will produce more severe loads throughout the inflation process. Overdesign weight is a useful test approach but it should be understood that the shape of the decelerator at the time of peak load will change, thereby shifting the location of maximum stress and changing its value.
- Overdesign opening load provides a rather good indication of the capability of longitudinal risers and lines, and of radial-decelerator members. However, unless an overdesign-opening-load test is designed with care and unless a full expansion of the canopy is produced, the test may not prove that the structure has been subjected to the desired maximum circumferential stress. There is some risk that an excessively conservative design, motivated by the desire to facilitate passing ultimate-strength tests, may result in unnecessary overstructure and, consequently, a substantial weight penalty. The risk that test conditions will adversely govern decelerator design can be minimized either by performing tests at less than ultimate-load conditions or by obtaining the agreement of everyone concerned that extensive structural damage in an ultimate-load test is acceptable. An alternate recommendation is to perform preliminary overload tests with minimum-weight models to identify critical areas by the incidence of damage. Then added weight can be kept to a minimum by making reinforcements only in these local areas.

Tests should be designed to provide the best possible simulation of unusual environments (e.g., extreme altitude, sterilization, etc.) or such poorly defined environments as the atmospheres of the planets Mars and Venus, and of Titan (the largest of Saturn's nine moons). The requirements for flight and other types of tests giving good simulation of specific conditions can be determined with the aid of the scaling laws described in references 69 and 70. It should be recognized that complete simulation of all parameters in a single test is generally not possible, due to mismatches of Mach number, Reynolds number, Froude number, etc. Environmental tests of material samples are necessary but are generally not adequate to ascertain all pertinent effects. Complete decelerator packs should be thoroughly preconditioned in the simulated design environment before making critical functional and performance tests (ref. 11); the operational time sequence of exposure and deployment should be duplicated as nearly as possible (ref. 58).

Dynamic tests should be performed and variable strain-rate data gathered for both material specimens and decelerator subassemblies when such members will be subjected to high onset shocks during system deployment and operation. Existing dynamic data from tests of both aircraft-cargo harness and personnel-safety harness should be used as applicable.

REFERENCES

1. Murray, H. L.: Parachute Subsystem Apollo Block II Increased Capability Earth Landing System – Final Report of the Series 85 Qualification Drop Tests. Vols. I and II, Rept. NVR-6070, Northrop Corp., Aug. 1968.
2. Buhler, W. C.: Installation, Operation and Maintenance – Project Mercury Landing System and Post Landing Equipment. Rept. RP-2201B, Northrop Corp., Aug. 1960.
3. Ewing, E. G.; and Vickers, J. R.: Feasibility Study of a Universal Aerial Recovery System. Vol. I, AFSSD-TR-66-47, Northrop Corp., Apr. 1966.
4. Anon.: Design Development of a Universal Aerial Recovery System – Phase III (Product Improvement). AFSAMSO-68-244, Northrop Corp., June 1968.
5. McClow, J. H.: Preliminary Development Testing of 53 ft. Parachute with Conical Extension for Aerial Retrieval. AFSSD-TR-66-204, Aerospace Corp., Nov. 1966.
6. Anon.: Development of a Single Conical Extension Parachute for Project Prime (U). Final Rept. GER-12802, Goodyear Aerospace Corp., Sept 1966. (Confidential)
7. Chernowitz, G., ed.: Performance and Design Criteria for Deployable Aerodynamic Decelerators. ASD-TR-61-579, AF Flight Dynamics Laboratory, Wright-Patterson AFB, Ohio, Dec. 1963.
8. Mikulas, M. M., Jr.; and Bohon, H. L.: Summary of the Development Status of Attached Inflatable Decelerators. Paper no. 68-929, presented at AIAA Second Aerodynamic Deceleration Systems Conference (El Centro, Calif.), Sept. 1968.
9. Gillis, C. L.: Aerodynamic Deceleration Systems for Space Missions. J. Spacecraft Rockets, vol. 6, no. 8, Aug. 1969, pp. 885-890.
10. Alexander, W. C.; and Lau, R. A.: State-of-the-Art Study for High Speed Deceleration and Stabilization Devices. NASA CR-66141, 1966.

11. Murrow, H. N.; and McFall, J. C., Jr.: Summary of Experimental Results Obtained from the NASA Planetary Entry Parachute Program. Paper no. 68-934, presented at AIAA Second Aerodynamic Deceleration Systems Conference (El Centro, Calif.), Sept. 1968.
12. Pepper, W. B., Jr.: Parachute Design and Performance for Supersonic Deployment and for the Recovery of Heavy Loads. Rept. SC-DC-69-1883, Sandia Lab., Sept. 1969.
13. Moeller, J. H.; Linhart, E. M.; Gran, W. M.; and Parson, L. T.: Free Flight Investigation of Large All-Flexible Parawings. NASA CR-66918, 1970.
14. Ranes, R. L.; Mullins, W. M.; Lindh, K. G.; McIntire, J. H.; and McEwan, A. J.: Optimum Structural Design of a Large All-Flexible Parawing. Rept. NVR-6478, Northrop Corp., Nov. 1969.
15. Bloetscher, F.: Aerodynamic Deployable Decelerator Performance -- Evaluation Program -- Phase II. AFFDL-TR-67-25, Goodyear Aerospace Corp., June 1967.
16. Bloetscher, F.; and Arnold, W. V.: Aerodynamic Deployable Decelerator Performance -- Evaluation Program -- Phase III. AFFDL-TR-67-60, Goodyear Aerospace Corp., June 1967.
17. Anon.: Voyager Decelerator 37-Foot Diameter Full Scale Drop Test. Rept. GER-13577, Goodyear Aerospace Corp., Dec. 1967.
18. Levin, A. D.; and Smith, R. C.: Experimental Aerodynamics of a Rotor Entry Vehicle. Paper no. 68-950, presented at AIAA Second Aerodynamic Deceleration Systems Conference (El Centro, Calif.), Sept. 1968.
19. Himmel, N. S.: Earth-Landing Rotor Spacecraft Studies. Aviation Wk. and Space Technol., vol. 90, no. 16, Apr. 21, 1969, p. 51.
20. Smith, R. C.; and Levin, A. D.: The Unpowered Rotor: A Lifting Decelerator for Spacecraft Recovery. Paper no. 68-969, presented at AIAA Second Aerodynamic Deceleration Systems Conference (El Centro, Calif.), Sept. 1968.
21. Barzda, J. J.: Rotary Wing Decelerators. Proc. Symposium on Parachute Technology and Evaluation, FTC TDR-64-12, Vol. I, AF Flight Test Center, Edwards AFB, Calif., Sept. 1964, pp. 66-87.

22. Scher, S. H.; and Dunavent, J. C.: Preliminary Analytical Study of Booster Recovery by Means of a Drag Balloon Which Converts to a Hot-Air Balloon for Final Recovery. Proc. AIAA Aerodynamic Deceleration Systems Conference (Houston, Tex.), Sept. 1966, pp. 165-171.
23. Greensite, A. L.: Abort. Vol. XVI of Analysis and Design of Space Vehicle Flight Control Systems. NASA CR-835, 1969.
24. Pedersen, P. E.: Study of Parachute Performance and Design Parameters for High Dynamic Pressure Operation. AFFDL-TDR-64-66, Wright-Patterson AFB, Ohio, May 1964.
25. Lowry, J. F.: Aerodynamic Characteristics of Various Types of Full Scale Parachutes at Mach Numbers from 1.8 to 3.0 (U). Rept. AEDG-TDR-64-120, Propulsion Wind Tunnel Facility, ARO, Inc., June 1964 (Confidential)
26. Nickel, W. E.; and Sims, L. W.: Study and Exploratory Free-Flight Investigation of Deployable Aerodynamic Decelerators Operating at High Altitudes and at High Mach Numbers. Vol. I, AFFDL-TDR-64-35, Wright-Patterson AFB, Ohio, July 1964.
27. Nebiker, F. R.: Aerodynamic Deployable Decelerator Performance Evaluation Program. AFFDL-TR-65-27, Goodyear Aerospace Corp., Aug. 1965.
28. Pepper, W. B.: Development of a Composite Structure Hypersonic Parachute. Paper no. 68-963, presented at AIAA Second Aerodynamic Deceleration Systems Conference (El Centro, Calif.), Sept. 1968.
29. Nerem, R. M.; and Henke, D. W.: Theoretical and Experimental Studies of Supersonic Turbulent Wakes and Parachute Performance. Paper no. 68-947, presented at AIAA Second Aerodynamic Deceleration Systems Conference (El Centro, Calif.), Sept. 1968.
30. Alexander, W. C.: A Discussion of Governing Decelerator Performance and Design Parameters in the Supersonic Flight Regime. Paper no. 68-938, presented at AIAA Second Aerodynamic Deceleration Systems Conference (El Centro, Calif.), Sept. 1968.
31. Knacke, T. W.: The Apollo Parachute Landing System. NV Tech. Publication 131, Northrop Corp., presented at AIAA Second Aerodynamic Deceleration Systems Conference (El Centro, Calif.), Sept. 1968.

32. Riffle, A. B.: Determination of the Aerodynamic Drag and Static Stability of Reefed Parachute Canopies (Wind Tunnel Study). AFFDL-TR-64-166, Wright-Patterson AFB, Ohio, Jan. 1965.
33. Pranger, R. J.: Missile and Target Recovery Parachutes. AFFTC-TR-60-31, ARDC, Oct. 1960.
34. Ewing, E. G.: Design Analysis — 128.8 ft D_O Century Ringsail (Project 1821). Rept. NVR-4051, Northrop Corp., June 1966.
35. Ewing, E. G.: Development Program for a Ringsail Parachute (Century Series) Final Report. Rept. NVR-5028, Northrop Corp., Dec. 1966.
36. Ewing, E. G.: Lightweight Parachute Design Criteria Applied to Improve Ringsail Structural Efficiency. Rept. NVR-4098, Northrop Corp., Nov. 1966.
37. Boettcher, E. W.; and Hanson, G. P.: Planetary Entry Parachute Program Cross Parachute Engineering Design Report. NASA CR-66590, 1967
38. Norman, L. C.; McCullough, J. E.; and Coffey, J. C.: Full-Scale Investigations. Vol. I, Gemini Land Landing System Development Program, NASA TN D-3869, 1967.
39. Norman, L. C.; McCullough, J. E.; and Coffey, J. C.: Supporting Investigations. Vol. II, Gemini Land Landing System Development Program, NASA TN D-3870, 1967.
40. Graham, C. R.; Riley, V. F.; and Linhart, E. M.: Investigation of Various Textile Parachutes and Control Systems to Achieve Steerability. Phase II, AFFDL-TDR-64-81, Pt. II, June 1965; Phases III and IV, AFFDL-TDR-64-81, Pt. III, Jan. 1966.
41. Linhart, E. M.; and Buhler, W. C.: Wind Tunnel and Free Flight Investigation of All-Flexible Parawings at Small Scale. NASA CR-66879, 1969.
42. Sleeman, W. C., Jr.; and Gainer, T. G.: Status of Research on Parawing Lifting Decelerators. Paper no. 68-967, presented at AIAA Second Aerodynamic Deceleration Systems Conference (El Centro, Calif.), Sept. 1968.
43. Barte, G. R., Jr.: Flexible Wings for Maneuvering and Landing Application in the De-Coupled Concept. AIAA Paper no. 67-200, presented at Fifth Aerospace Sciences Meeting (New York), Jan. 23-26, 1967.

44. Ware, G. M.; and Libbey, C. E.: Wind Tunnel Investigation of the Static Aerodynamic Characteristics of a Multi-Lobe Gliding Parachute. NASA TN D-4672, 1968.
45. Speelman, R. J., III; Pepper, W. B.; and Menard, G. L. C.: A Review of Para-Foil Programs. Paper no. 68-968, presented at AIAA Second Aerodynamic Deceleration Systems Conference (El Centro, Calif.), Sept. 1968.
46. Knapp, C. F.; and Barton, W. R.: Controlled Recovery of Payloads at Large Glide Distances, Using the Para-Foil. Rept. SC-R-67-1049, Sandia Lab., Nov. 1967.
47. Nerem, R. M.: Pressure and Heat Transfer on High-Speed Aerodynamic Decelerators of the Ballute Type. Proc. AIAA Aerodynamics Deceleration Systems Conference (Houston, Tex.), Sept. 1966, pp. 135-143.
48. Heinrich, H. G.; and Hess, R. S.: Drag Characteristics of Plates, Cones, Spheres and Hemispheres in the Wake of a Forebody at Transonic and Supersonic Speeds. RTD-TDR-63-4242, Air Force Flight Dynamics Laboratory, Wright-Patterson AFB, Ohio, Dec. 1964.
49. Hoerner, S. F.: Fluid Dynamic Drag. Published by author, Library of Congress catalog no. 64-19666, 1965.
50. Guy, L. D.: Structural and Decelerator Design Options for Mars Entry. Paper no. 68-344, presented at AIAA/ASME Ninth Structures, Structural Dynamics, and Materials Conference (Palm Springs, Calif.), Apr. 1968.
51. Knacke, T. W.; Paulson, K. R.; and Schurr, G. G.: Study of Self Recovery. AFOSR-104, Air Force Office of Scientific Research, Mar. 1961.
52. Anon.: The F-111 Crew Module. Rept. FZM-12-4094A, General Dynamics Corp., Nov. 1966.
53. Lofland, W. W.: Program Report on Sailwing. Paper no. 68-966, presented at AIAA Second Aerodynamic Deceleration Systems Conference (El Centro, Calif.), Sept. 1968.
54. Swanson, J. N.; and Dedon, W. W.: Flight Qualification Test Program — Gemini Parachute Landing System — Spacecraft 3 Configuration. Rept. NVR 3796, Northrop Corp., July 1965.
55. French, K. E.: Model Law for Parachute Opening Shock. AIAA J., vol. 2, no. 12, Dec. 1964, pp. 2226-2228.

56. Dayman, B., Jr.; and Kurtz, D. W.: Forebody Effects on Drogue Drag in Supersonic Flow. Paper no. 68-8, presented at AIAA Sixth Aerospace Sciences Meeting (New York), Jan. 1968.
57. Henke, D. W.: Analysis of High Speed Axisymmetric Wakes and Parasonic Parachute Performance. Vol. II, Establishment of an Unsymmetrical Wake Test Capability for Aerodynamic Decelerators, AFFDL-TR-67-192, Mar. 1968.
58. Spence, D. C.: Effects of Mission Environments on the Mechanical Properties of Dacron Parachute Material. Paper no. L-6706, presented at AIAA/ASTM/IES Fourth Space Simulation Conference (Los Angeles), Sept. 1969.
59. Eckstrom, C. V.: Flight Tests of a 40-Foot-Nominal-Diameter Disk-Gap-Band Parachute Deployed at a Mach Number of 3.31 and a Dynamic Pressure of 10.6 Pounds per Square Foot. NASA TM X-1924, 1970.
60. Anon.: Study of Pressure Packing Techniques for Parachutes. ASD-TR-61-426, June 1962.
61. Anon.: Properties of DuPont Filament Yarns for Industrial Purposes. DuPont Bulletin X-219, Sept. 1967.
62. Anon.: Properties of Nomex — High Temperature Resistant Nylon Fiber. DuPont Bulletin N-201, Oct. 1966.
63. Alexander, W. C.: Investigation to Determine the Feasibility of Using Inflatable Balloon-Type Drag Devices for Recovery Applications in the Transonic, Supersonic and Hypersonic Flight Regimes. Pt. II, ASD-TDR-62-702, Goodyear Aerospace Corp., Oct. 1962.
64. Roper, W. D.: Effects of Decontamination, Sterilization and Thermal Vacuum on Spacecraft Polymeric Products. Tech. Rept. 32-1411, Jet Propulsion Lab., Calif. Inst. of Technol., June 1969.
65. Lashbrook, R. V.; and Mabry, C. M.: An Investigation of Low Permeability Fabrics and of Suspension and Control Lines for the All-Flexible Parawing. Paper no. 68-953, presented at AIAA Second Aerodynamic Deceleration Systems Conference (El Centro, Calif.), Sept. 1968.
66. DeMario, W. F.; and Lashbrook, R. V.: Effects of Heat on a Nylon Fabric. Rept. NVR-4028, Northrop Corp., Mar. 1966.

67. Schulman, S.: Tensile Properties of Fibrous Materials at Standard Conditions and Vacuum at Elevated Temperatures. Paper no. 68-954, presented at AIAA Second Aerodynamic Deceleration Systems Conference (El Centro, Calif.), Sept. 1968.
68. Opt, P. C.: Tensile Impact Behavior at Elevated Temperatures of Webbing, Tapes and Ribbons for Decelerators. Paper no. 68-952, presented at AIAA Second Aerodynamic Deceleration Systems Conference (El Centro, Calif.), Sept. 1968.
69. Barton, R. L.: Scale Factors for Parachute Opening. NASA TN D-4123, 1967.
70. Mickey, F. E.; Ewing, E. G.; McEwan, A. J.; and Huyler, W. C., Jr.: Loads. Vol. I, Investigation of Prediction Methods for the Loads and Stresses of Apollo Type Spacecraft Parachutes. Rept. NVR-6431, Northrop Corp., June 1970.
71. Moeller, J. H.: A Method of Load Prediction for Parachutes in Cluster. Proc. AIAA Aerodynamic Deceleration Systems Conference (Houston, Tex.), Sept. 1966, pp. 64-72.
72. Mullins, W. M.; Reynolds, D. T.; Bottorff, M. R.; and Lindh, K. G.: Stresses. Vol. II, Investigation of Prediction Methods for the Loads and Stresses of Apollo Type Spacecraft Parachutes. Rept. NVR-6432, Northrop Corp., June 1970.
73. Greene, G. C.: Opening Distance of a Parachute. J. Spacecraft Rockets, vol. 7, no. 1, Jan. 1970, pp. 90-100.
74. White, F. M.; and Wolf, D. F.: A Theory of Three-Dimensional Parachute Dynamic Stability. Proc. AIAA Aerodynamic Deceleration Systems Conference (Houston, Tex.), Sept. 1966, pp. 33-46.
75. Heinrich, H. G.; and Jamison, L. R., Jr.: Parachute Stress Analysis During Inflation and at Steady State. Aircraft, vol. 3, no. 1, Jan.-Feb. 1966, pp. 52-58.
76. Scheubel, F. N.: Notes on Opening Shock of a Parachute. Progress Rept. IRE-65, Foreign Exploitation Section, Intelligence (T-2), Apr. 1946.
77. Rust, L. W., Jr.: Theoretical Investigation of the Parachute Inflation Process. Rept. NVR 3887, Northrop Corp., July 1965.
78. Heinrich, H. G.; and Noreen, R. A.: Analysis of Parachute Opening Dynamics With Supporting Wind Tunnel Experiments. Paper no. 68-924, presented at AIAA Second Aerodynamics Deceleration Systems Conference (El Centro, Calif.), Sept. 1968.

79. Neustadt, M.; Ericksen, R. E.; Guiteras, J. J.; and Larrivee, J. A.: A Parachute Recovery System Dynamic Analysis. AIAA Paper no. 66-25, AIAA Third Aerospace Sciences Meeting (New York), Jan. 24-26, 1966.
80. Smetana, R. O.; and Miller, D. C.: The Effects of Variations in Altitude on the Opening Shock and Stability of Parachutes. Paper no. 68-926, presented at AIAA Second Aerodynamic Deceleration Systems Conference (El Centro, Calif.), Sept. 1968.
81. Melzig, H. D.; and Soliaris, C.: Pressure Distribution During Parachute Opening – Finite Mass Operating Case – Phase II. AFFDL-TR-68-135 Wright-Patterson AFB, Ohio, Feb. 1969.
82. Timoshenko, S.; and Woinowsky-Krieger, S.: Theory of Plates and Shells. McGraw-Hill Book Co., Inc., 1959.
83. McFall, J. C.; and Murrow, H. N.: Parachute Testing at Altitudes Between 30 and 90 Kilometers. Proc. AIAA Aerodynamic Deceleration Systems Conference (Houston, Tex.), Sept. 1968, pp. 116-121.
84. Huckins, E. K., III: Techniques for Selection and Analysis of Parachute Deployment Systems. NASA TN D-5619, 1970
85. Kuchta, B. J.: Dynamic Stability of Space Vehicles. Vol. XII, Re-Entry Vehicle Landing Ability and Control. NASA CR-946, 1968.
86. Mileaf, H.: Handbook of Fibrous Materials. WADD TR 60-584, McGraw-Hill Book Co., Inc., 1960.
87. Anderson, M. S.; Bohon, H. L.; and Mikulas, M. M., Jr.: A Structural Merit Function for Aerodynamic Decelerators. NASA TN D-5535 1969.

SYMBOLS

A_p	allowable strength factor
b_w	nominal wing span
C_D	drag coefficient, general
C_{D_o}	drag coefficient based on area S_o
C_K	opening-load factor (formerly known as opening-shock factor, X)
C_L	lift coefficient, general
C_M	pitching-moment coefficient
C_N	normal-force coefficient
C_T	tangent-force coefficient
D	drag or diameter, general
D_o	nominal diameter of parachute $(4S_o/\pi)^{1/2}$
D_p	inflated diameter (projected)
D_R	diameter of reefing-line circle (ℓ_R/π)
d_B	diameter of body
E_n	Euler number $(F_o/S_o q_1)$
F	structural load; force, general
F_n	Froude number $(gD_o \sin \gamma / v_1^2)$
F_o	opening force

F_s	snatch force
F_{ult}	ultimate load, breaking strength
g	acceleration of gravity
K	constant, general; spring constant
K_a	added mass shape factor
K_f	filling interval, dimensionless
L	lift
ℓ	length of control line; length, general
ℓ_R	length of reefing line
ℓ_s	length of suspension line
$\Delta\ell$	control-line displacement distance
M	system (vehicle + decelerator) mass; also for Mach number
m	mass, general
m_a	added air mass
P_A	allowable strength
P_R	rated strength
P'_R	required strength
p	pressure, general
Δp	differential pressure
q	dynamic pressure, general
q_1	dynamic pressure at start of filling process
R_m	mass ratio ($\rho\psi^{3/2}/M$)

r	radius, general
r_c	radius of curvature
S	area, general
S_o	nominal area of drag surface, including vents and slots
S_w	area of lifting surface
T	unit tensile load
T_c	circumferential-unit tensile load
Δt_f	filling time
v_H	horizontal velocity
v_1	velocity at start of filling process
v_V	vertical velocity, "sinking speed"
Δv	differential velocity
W	gross weight of system (vehicle + decelerator)
W_p	weight of parachute
W_w	weight of deployable wing
X	opening-shock factor (now known as opening-load factor, C_K)
x	decelerator trailing distance
z	number of identical members
α	angle of attack
β	angle of turn
$\dot{\beta}$	rate of turn
γ	flight-path angle

ϵ	elongation distance
θ	angle of axial deflection from tangent ($\theta \cong 90 \text{ deg} - \alpha$)
λ_m	material or fabric porosity
λ_T	total porosity
ρ	air density
Σ	summation
σ	standard deviation
ψ	effective drag area ($\equiv C_D S$)

ABBREVIATIONS

D.F. design factor

M.S. margin of safety

S.F. safety factor

NASA SPACE VEHICLE DESIGN CRITERIA MONOGRAPHS ISSUED TO DATE

SP-8001	(Structures)	Buffeting During Atmospheric Ascent, May 1964 – Revised November 1970
SP-8002	(Structures)	Flight-Loads Measurements During Launch and Exit, December 1964
SP-8003	(Structures)	Flutter, Buzz, and Divergence, July 1964
SP-8004	(Structures)	Panel Flutter, July 1964
SP-8005	(Environment)	Solar Electromagnetic Radiation, June 1965 – Revised May 1971
SP-8006	(Structures)	Local Steady Aerodynamic Loads During Launch and Exit, May 1965
SP-8007	(Structures)	Buckling of Thin-Walled Circular Cylinders, Sep- tember 1965 – Revised August 1968
SP-8008	(Structures)	Prelaunch Ground Wind Loads, November 1965
SP-8009	(Structures)	Propellant Slosh Loads, August 1968
SP-8010	(Environment)	Models of Mars Atmosphere (1967), May 1968
SP-8011	(Environment)	Models of Venus Atmosphere (1968), December 1968
SP-8012	(Structures)	Natural Vibration Modal Analysis, September 1968
SP-8013	(Environment)	Meteoroid Environment Model – 1969 [Near Earth to Lunar Surface], March 1969
SP-8014	(Structures)	Entry Thermal Protection, August 1968
SP-8015	(Guidance and Control)	Guidance and Navigation for Entry Vehicles, No- vember 1968
SP-8016	(Guidance and Control)	Effects of Structural Flexibility on Spacecraft Control Systems, April 1969
SP-8017	(Environment)	Magnetic Fields – Earth and Extraterrestrial, March 1969
SP-8018	(Guidance and Control)	Spacecraft Magnetic Torques, March 1969
SP-8019	(Structures)	Buckling of Thin-Walled Truncated Cones, Sep- tember 1968
SP-8020	(Environment)	Mars Surface Models (1968), May 1969
SP-8021	(Environment)	Models of Earth's Atmosphere (120 to 1000 km), May 1969

SP-8022	(Structures)	Staging Loads, February 1969
SP-8023	(Environment)	Lunar Surface Models, May 1969
SP-8024	(Guidance and Control)	Spacecraft Gravitational Torques, May 1969
SP-8025	(Chemical Propulsion)	Solid Rocket Motor Metal Cases, April 1970
SP-8026	(Guidance and Control)	Spacecraft Star Trackers, July 1970
SP-8027	(Guidance and Control)	Spacecraft Radiation Torques, October 1969
SP-8028	(Guidance and Control)	Entry Vehicle Control, November 1969
SP-8029	(Structures)	Aerodynamic and Rocket-Exhaust Heating During Launch and Ascent, May 1969
SP-8030	(Structures)	Transient Loads from Thrust Excitation, February 1969
SP-8031	(Structures)	Slosh Suppression, May 1969
SP-8032	(Structures)	Buckling of Thin-Walled Doubly Curved Shells, August 1969
SP-8033	(Guidance and Control)	Spacecraft Earth Horizon Sensors, December 1969
SP-8034	(Guidance and Control)	Spacecraft Mass Expulsion Torques, December 1969
SP-8035	(Structures)	Wind Loads During Ascent, June 1970
SP-8036	(Guidance and Control)	Effects of Structural Flexibility on Launch Vehicle Control Systems, February 1970
SP-8037	(Environment)	Assessment and Control of Spacecraft Magnetic Fields, September 1970
SP-8038	(Environment)	Meteoroid Environment Model – 1970 (Interplane- tary and Planetary), October 1970
SP-8040	(Structures)	Fracture Control of Metallic Pressure Vessels, May 1970
SP-8041	(Chemical Propulsion)	Captive-Fired Testing of Solid Rocket Motors, March 1971
SP-8042	(Structures)	Meteoroid Damage Assessment, May 1970
SP-8043	(Structures)	Design-Development Testing, May 1970
SP-8044	(Structures)	Qualification Testing, May 1970
SP-8045	(Structures)	Acceptance Testing, April 1970
SP-8046	(Structures)	Landing Impact Attenuation for Non-Surface- Planing Landers, April 1970
SP-8047	(Guidance and Control)	Spacecraft Sun Sensors, June 1970

SP-8048	(Chemical Propulsion)	Liquid Rocket Engine Turbopump Bearings, March 1971
SP-8050	(Structures)	Structural Vibration Prediction, June 1970
SP-8051	(Chemical Propulsion)	Solid Rocket Motor Igniters, March 1971
SP-8053	(Structures)	Nuclear and Space Radiation Effects on Materials, June 1970
SP-8054	(Structures)	Space Radiation Protection, June 1970
SP-8055	(Structures)	Prevention of Coupled Structure-Propulsion Instability (Pogo), October 1970
SP-8056	(Structures)	Flight Separation Mechanisms, October 1970
SP-8057	(Structures)	Structural Design Criteria Applicable to a Space Shuttle, January 1971
SP-8058	(Guidance and Control)	Spacecraft Aerodynamic Torques, January 1971
SP-8059	(Guidance and Control)	Spacecraft Attitude Control During Thrusting Maneuvers, February 1971
SP-8060	(Structures)	Compartment Venting, November 1970
SP-8061	(Structures)	Interaction with Umbilicals and Launch Stand August 1970
SP-8062	(Structures)	Entry Gasdynamic Heating, January 1971
SP-8063	(Structures)	Lubrication, Friction, and Wear, June 1971
SP-8066	(Structures)	Deployable Aerodynamic Deceleration Systems, June 1971
SP-8068	(Structures)	Buckling Strength of Structural Plates, June 1971
SP-8072	(Structures)	Acoustic Loads Generated by the Propulsion System, June 1971

NATIONAL AERONAUTICS AND SPACE ADMINISTRATION

WASHINGTON, D. C. 20546

OFFICIAL BUSINESS

PENALTY FOR PRIVATE USE \$300

FIRST CLASS MAIL



POSTAGE AND FEES PAID
NATIONAL AERONAUTICS AND
SPACE ADMINISTRATION

POSTMASTER: If Undeliverable (Section 138
Postal Manual) Do Not Return
